

**TRANSIENT VARIATIONS OF THERMAL STRESSES AND THE
RESULTING RESIDUAL STRESSES WITHIN A THIN PLATE DURING
WELDING PROCESSES**

2000
2000
2000

By
Maher A. Da'as

تعتمد كلية الدراسات العليا
هذه النسخة من الرسالة
التوقيع..... التاريخ.....

Supervisor

Dr. Naser S. Al-Huniti

Co-Supervisor

Dr. Mohammed A. Al-Nimr

Submitted in Partial fulfillment of the Requirements

For the degree of Master of Science in

Mechanical Engineering

Faculty of Graduate Studies

University of Jordan

2000
2000

August 2000

This thesis was successfully defended and approved on ..August, 10, 2000

Examination Committee

Signature

Dr. Naser S. Al-Huniti, Chairman
Assis. Prof. of Applied Mechanics

Naser Al-Huniti 23/8/2000

Dr. Mohammed Al-Nimr, Member
Assoc. Prof. of Thermal Mechanics

Moh'd Al-Nimr 9/22

Dr. Sa'ad S. Al-Habali, Member
Prof. of Applied Mechanics

S. Habale 23.8.2000

Dr. Osama Abu Zeid, Member
Assis. Prof. of Applied Mechanics

Osama Abu Zeid 23.8.2000

Dr. Mohammed Alkam, Member
Assis. Prof. of Thermal Mechanics

M. Alkam 8/23/2000

DEDICATION

To My Parents

Brothers, Sister and My Wife

ACKNOWLEDGEMENTS

I gratefully acknowledge *Dr. Naser Al-Huniti* and *Dr. Moh'd Al-Nimr* for their suggestions and continuous encouragement at every stage of my work. I am also grateful to the examination committee members for their efforts. Special thanks are owed to all those who helped and supported me throughout this work. Furthermore, I wish to thank *Mrs. Tamara Abed Al-Kareem* for her effective cooperation and great care taken in editing this work in this manner.

TABLE OF CONTENTS

EXAMINATION COMMITTEE DECISION	ii
DEDICATION	iii
ACKNOWLEDGMENTS	iv
TABLE OF CONTENTS	v
LIST OF FIGURES	vii
NOMENCLATURE	ix
GREEK LETTERS	x
LIST OF APPENDICES	xi
ABSTRACT	xii
CHAPTER ONE	
INTRODUCTION AND LITERATURE REVIEW	1
1.1 Introduction	1
1.2 Literature Review	2
1.3 Objective of the Present Work	6
1.4 Organization of the Thesis	6
CHAPTER TWO	
MATHEMATICAL FORMULATION AND SOLUTION OF THE	8
HEAT CONDUCTION MODEL	
2.1 Introduction	8
2.2 Assumptions	9
2.3 Derivation of the Governing Equation	10

CHAPTER THREE	
DETERMINATION OF THERMAL AND RESIDUAL STRESSES	20
3.1 Introduction	20
3.2 Physical Properties	20
3.3 Thermal Stresses	24
3.4 Residual Stress	27
3.5 Computation of Thermal and Residual Stress	28
CHAPTER FOUR	
RESULTS AND DISCUSSION	32
4.1 Introduction	32
4.2 Numerical Data	32
4.3 Results and Discussion	34
CHAPTER FIVE	
CONCLUSIONS AND RECOMMENDATIONS	48
5.1 Conclusions	48
5.2 Recommendations	50
REFERENCES	51
APPENDIX A	53
APPENDIX B	56
APPENDIX C	57
APPENDIX D	60
ABSTRACT IN ARABIC	63

LIST OF FIGURES

Figure(2.1.1)	3-D thin plate and heat source	8
Figure(2.3.1)	Finite element on the plate	10
Figure(3.2.1)	Modulus of elasticity for mild steel	21
Figure(3.2.2)	Yield stress for mild steel	22
Figure(3.2.3)	Coefficient of linear thermal expansion for mild steel	23
Figure(3.3.1)	Schematic representation of changes of temperature and stresses during welding	26
Figure(4.3.1)	Temperature changes at different longitudinal lines	38
Figure(4.3.2)	Stress changes at different longitudinal lines	39
Figure(4.3.3)	Residual stress distribution inside the plate	40
Figure(4.3.4)	Thermal cycles at different transverse lines	41
Figure(4.3.5)	Temperature changes at different input heat intensities	42
Figure(4.3.6)	Residual stress distributions inside the plate at different input heat intensities	43
Figure(4.3.7)	Temperature changes at different weld speeds	44
Figure(4.3.8)	Residual stress distributions inside the plate at different weld speeds	45

Figure(4.3.9)	Temperature changes at different thicknesses	46
Figure(4.3.10)	Residual stress distributions inside the plate at different thicknesses	47

529020

NOMENCLATURE

C	Specific heat
E	Modulus of elasticity
g, g_0	Heat source per unit length
G_0	Dimensionless heat source
h_u	Upper surface heat convection coefficient
h_l	lower surface heat convection coefficient
K	Thermal conductivity
H	Length of the plate
$2L$	Width of the plate
Q	Heat flux
R	Aspect ratio
t, t_0	Time
T	Plate temperature
T_∞	Ambient temperature
V	Dimensionless heat source velocity
\bar{V}	Heat source velocity
w	Plate thickness
W	Dimensionless temperature
x, y, z	Spatial coordinates

GREEK LETTERS

α	Diffusivity
β_i	Dimensionless parameter
β_m	Eigenfunction
γ	Dimensionless parameter
δ	Unit step function
ε_n	Eigenfunction
η	Dimensionless coordinate in longitudinal direction
θ	Dimensionless temperature
ρ	Density
ζ	Dimensionless coordinate in transverse direction
σ	Stress
τ	Time
ψ	Dimensionless temperature

LIST OF APPENDICES

APPENDIX A:

COMPUTER PROGRAM FOR CALCULATING THE 53
TEMPERATURE DISTRIBUTION AT DIFFERENT TIMES

APPENDIX B:

COMPUTER PROGRAM FOR CALCULATING THE 56
PHYSICAL PROPERTIES AT DIFFERENT TEMPERAURE
VALUES

APPENDIX C:

COMPUTER PROGRAM FOR CALCULATING THE 57
TEMPERATURE DISTRIBUTION AT DIFFERENT TIMES
ALONG CERTAIN SECTION ON THE PLATE

APPENDIX D:

COMPUTER PROGRAM FOR CALCULATING THE 60
RESIDUAL STRESSES INSIDE THE THIN PLATE

ABSTARCT**TRANSIENT VARIATIONS OF THERMAL STRESSES AND THE
RESULTING RESIDUAL STRESSES WITHIN A THIN PLATE DURING
WELDING PROCESSES**

By

Maher A. Da'as

Supervisor

Dr. Naser S. Al-Huniti

Co-Supervisor

Dr. Mohammed A. Al-Nimr

Variations of thermal and residual stresses are investigated inside thin mild steel plate due to welding process. The temperature distribution due to heat transfer by conduction inside the plate with certain boundary conditions is found analytically. Then the transient thermal stresses developed are computed. The resulting residual stresses, which remain after cooling of the plate, are found using the method presented originally by Tall 1964 and the results are presented in graphical forms. It was found that welding speed and heat source intensity are the main factors affecting the residual stress formation.

CHAPTER ONE

INTRODUCTION AND LITERATURE REVIEW

1.1 Introduction

Weld is a localized coalescence of metals or non-metals produced either by heating the materials to suitable temperature with or without the application of pressure or by the application of the pressure alone and with or without the use of filler material. More than fifty different welding processes are now used commercially and can be classified into fusion welding (arc welding), electrical-resistance welding (spot welding), solid phase welding (pressure welding), liquid-solid phase joining (brazing and soldering) and adhesive bonding (cements).

Because a weldment is locally heated, the temperature distribution in the workpiece is not uniform and changes take place as welding progresses. The temperature of the base metal and weld metal in the vicinity of weld line (heat-affected zone or HAZ) is higher than that of the unaffected base metal. As the molten pool solidifies and shrinks, it begins to exert shrinkage stresses on the surrounding weld metal and heat affected zone area. After it cools to the surrounding ambient temperature, shrinkage of the metal causes stresses to form inside the plate. Part of these stresses will be recovered due to elasticity while the other part will remain (residual stresses). These residual stresses change the properties of the welded plate.

This leads to metal distortion and may cause premature failure in weldment.

1.2 Literature Review

Many researchers studied the temperature variation and the resulting thermal and residual stresses in welded plates. Tall (1964) presented a method for the calculation of thermal and residual stresses produced in individual plates due to welding. Comparison between theoretical and experimental residual stress distribution was also made. His method is a step-by-step method for the computation of the residual stresses arising in welded plates based on the knowledge of the temperature distribution obtained from an equation in the literature. Calculations were presented for both center-welded and edge welded structural steel plates and are compared with experimental results for the same plates.

Ueda and Yuan (1993) studied the characteristics of inherent strain distribution in butt welds by numerical experiments. Formulas were derived for the distribution and magnitude of inherent strain in a butt weld. A method for predicting the residual stress in a butt-welded plate using the characteristics of inherent strain distributions was presented. The validity of the method was demonstrated by thermal elasto-plastic analysis. It was found that the patterns vary little with changes in the welding conditions and sizes of the welded plates.

AL-Nimr and Abou Arab (1994) studied the transient heat conduction process with moving heat source/sink simulating the welding process. A closed form solution for the heat conduction equation was obtained. The temperature distribution was obtained and compared with numerical and experimental data in the literature. Despite of the assumptions used in their work, it was found that the obtained analytical solution has a satisfactory agreement with those used for comparison in the literature.

Ueda and Xing (1994) proposed a very simple measuring method for 3-dimensional residual stresses with the aid of distribution functions of inherent strains. In the simple measuring methods, inherent strain zones were predicted by newly proposed formulas based on the results of thermal elastic-plastic FEM analysis, and the coefficients involved in distribution functions of inherent strains are estimated using measured elastic strains at some points.

Yang and Xiao (1995) carried out an investigation to find an analytical model to examine the residual stress distribution across the weld of the panels welded with mechanical constraints. The panels to be welded were considered to be cantilever bars and the stress caused by the heat source during the welding process was assumed to have a parabolic distribution along the plate thickness. An ideal elastic-plastic material curve was assumed. As the depth of the yield zone increased, the position of the maximum stress shifted towards the bottom of the panel.

Antunes (1995) analyzed the basic aspects of the residual stresses in welding. Concepts about macro and micro residual stresses in metals were considered in welding. In a simple welding model, it was shown how shrinkage macro stress results and how this can contribute to understand the distribution of residual stresses in common types of welded joints. Further comments were made concerning the effects of additional mechanical and metallurgical phenomena, distortion in weldments and dimensional discrepancies.

Olabi and Hashmi (1995) presented some results on the effect of post-weld heat-treatment on the mechanical properties and residual stresses of I-beam welded box-section in structural steel material. In order to assess the effect of post-weld heat-treatment on the mechanical properties, microhardness, tensile strength and impact tests have been employed on the welded joint under two conditions: first, the as-welded condition: second, the as heat-treated condition. The hole-drilling method has been used to estimate the magnitude and distribution of residual stress before and after the application of post-weld heat treatment. The results showed that the post welded heat treatment (i) improve the toughness by about 15% without making any significant difference to the tensile strength and the hardness (ii) has the significant effect of reducing the residual stress by about 70%.

Roelens and Maltrud (1996) conducted a numerical modeling of submerged arc butt welding of 30 mm plates to determine residual stress

distribution after multipass welding. Comparisons of thermal cycles, sizes of heat affected zone and residual stresses were performed. Moreover X-rays powder diffraction and incremental hole drilling measurement were carried out to verify the numerical results. The transverse stress was correctly simulated; the comparison of the calculated stresses with the stresses obtained from the experiments yielded good qualitative and quantitative results.

Yaun and Ueda (1996) introduced a concept of inherent strain, being regarded as source of the residual stress in order to develop a predicting method of residual stresses in fillet T-and I-joints. With the proposed method the residual stress of an interested weldment may be predicted by performing an elastic analysis, in which the inherent strain is replaced to equivalent distributed loads. The inherent strain distributions in various T-and I-joints were investigated using numerical simulations. The results showed that the inherent strains distributing in flange side and in web side of the several joints are almost the same. The inherent strains vary not only with the average temperature rise due to welding, but with the geometric ratio of the joints.

In the present work, an arc welding process that combines two thin metal plates is simulated analytically. The temperature distribution inside the plate is found using the procedure used by Al-Nimr and Abou Arab (1994) but with different boundary conditions. The method presented by tall

(1964) was utilized and programmed but taking less time increments in order to increase accuracy. Tall studied the case of plate edge welding while plate center welding case is considered here.

1.3 Objectives of the Present Work:

In summary, this work presents a theoretical investigation of the thermal and stress behavior of a thin mild steel plate as a result of butt-welding. The main objectives of the present work are:

1. To formulate the energy balance equation for thin plate under certain boundary conditions and moving welding torch as a source of heat.
2. To solve the boundary value problem analytically to find a closed form solution that predicts the temperature distribution inside the plate at different times.
3. To calculate the transient thermal stresses developed due to welding process and also compute the residual stresses that remain in the thin plate after cooling.
4. To study the effect of welding speed, power input and other parameters on the formation of residual stresses inside the plate.

1.4 Organization of the thesis:

The thesis consists of five chapters. Chapter one is the introduction, in which the concepts of welding, thermal and transient stresses are

CHAPTER TWO

MATHEMATICAL FORMULATION AND SOLUTION OF THE HEAT CONDUCTION MODEL

2.1 Introduction

Figure (2.1.1) shows two identical rectangular thin metal plates to be joined together in butt welding process. The welding process is modeled as a moving heat source along the plates with constant velocity leaving a fusion zone behind the torch.

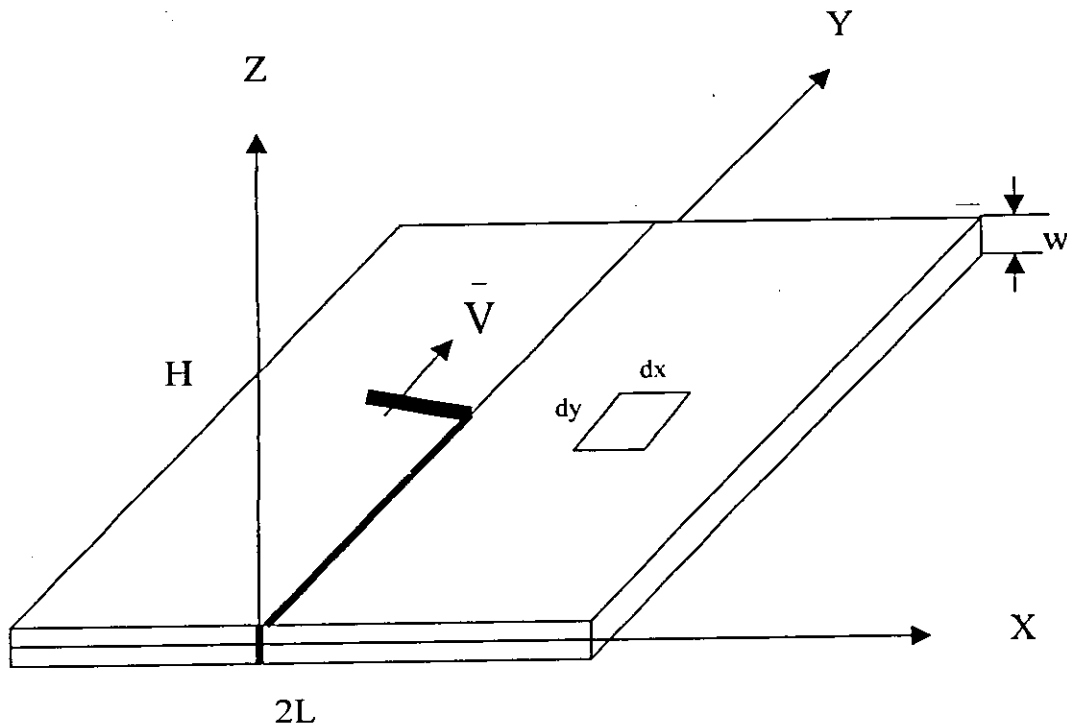


Figure (2.1.1) 3-D thin plate and heat source

Where

H: Length of the plate

2L: Width of the plate

w: Thickness of the plate

\bar{v} : Heat source velocity

2.2 Assumptions

The following assumptions are used in order to facilitate the derivation of temperature distribution equation.

1. The welding material fills between the two metal plates are thin (full penetration), this is the case for thin plates.
2. The heat source is a line heat source.
3. Welding material is deposited at a uniform rate in order to consider the heat source speed fixed during welding process.
4. The radiation loss from the sheets and weld are neglected to avoid sophisticated terms in heat conduction equation.
5. The material under consideration has constant thermal properties in the heat equation to avoid non-linear terms in conduction equation.

2.3 Derivation of the Governing Equation:

An analytical solution for the two-dimensional transient heat conduction problem is to be determined. The solution enables the determination of the effect of many welding parameters on the temperature distribution inside the thin plates at different times. The procedure used by Al-Nimr and Abou-Arab in 1994 is utilized to get the analytical solution, but the boundary and welding parameters are different.

The energy equation, which describes the present work heat conduction equation (see figure (2.3.1)), is:

$$\rho.Cdxdyw \frac{\partial T}{\partial t} = \left[q_x dy + q_y dx - \left(q_x dy + \frac{\partial q_x}{\partial x} dx dy \right) - \left(q_y dx + \frac{\partial q_y}{\partial y} dx dy \right) \right] .w - h_u(T - T_\infty)dx dy - h_l(T - T_\infty)dx dy + g_0 \delta(x) \delta(y - \bar{V} t) dx dy .w \quad (2.3.1)$$

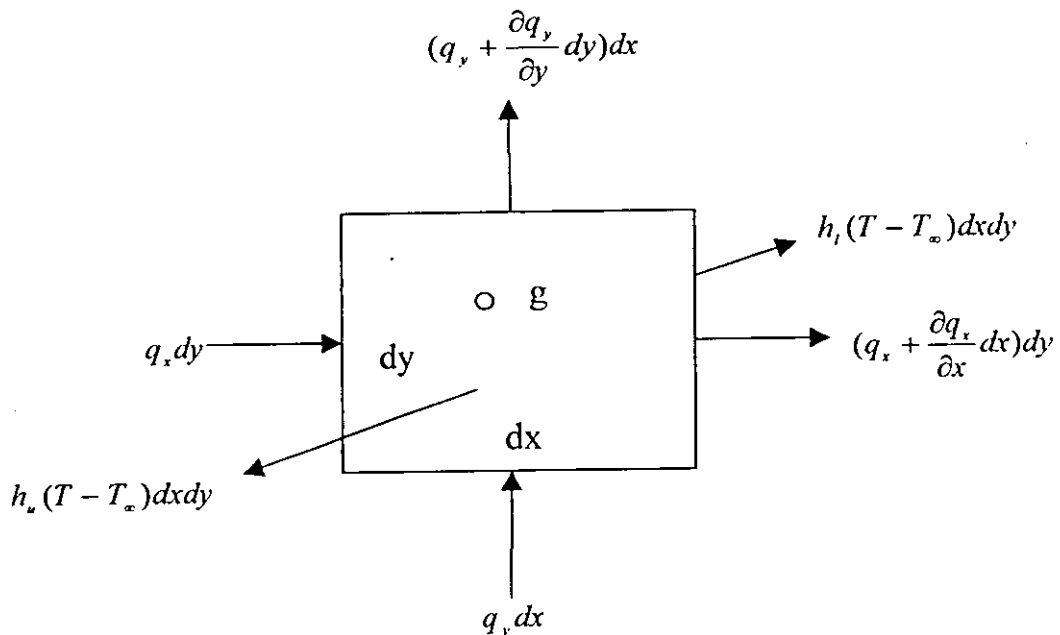


Figure (2.3.1) Finite element on the plate

Where:

- ρ : Density [kg/m^3]
 w : Thickness of the plate. [m]
 C : Specific heat [$\text{J}/(\text{kg}.\text{K})$]
 k : Thermal conductivity [$\text{W}/\text{m}.\text{K}$]
 h_l : Lower convection heat transfer coefficient [$\text{W}/\text{m}^2.\text{K}$]
 h_u : Upper convection heat transfer coefficient [$\text{W}/\text{m}^2.\text{K}$]
 T : Temperature at any location [K]
 T_∞ : Ambient temperature [K]
 g_0 : Heat generation per unit length [W/m].
 \bar{V} : Velocity of welding electrode [m/s].

The heat source is assumed to be moving along fixed x-point and moving in the y-direction so its location can be defined at $\delta(x)\delta(y - \bar{V}t)$.

Dividing equation (32.32.1) by $dx.dy.w$ gives:

$$\rho.C \frac{\partial T}{\partial t} = k \left[\frac{\partial^2 T}{\partial x^2} + \frac{\partial^2 T}{\partial y^2} \right] - \frac{h_u}{w} (T - T_\infty) - \frac{h_l}{w} (T - T_\infty) + g_0 \delta(x) \delta(y - \bar{V}t) \quad (2.3.2)$$

Initial and boundary conditions:

Initially, the plate temperature is assumed to be uniform and equal to the ambient temperature, the heat flux from the plate to the ambient is assumed

to be zero (insulated edges), so the initial and boundary conditions are as follows:

Initial condition:

$$T(0, x, y) = T_{\infty} \quad (2.3.2a)$$

Boundary conditions:

$$\text{At } x = 0 \quad \frac{\partial T}{\partial x} = 0 \quad (2.3.2b)$$

$$\text{At } x = L \quad \frac{\partial T}{\partial x} = 0 \quad (2.3.2c)$$

$$\text{At } y = 0 \quad \frac{\partial T}{\partial y} = 0 \quad (2.3.2d)$$

$$\text{At } y = H \quad \frac{\partial T}{\partial y} = 0 \quad (2.3.2e)$$

For the purpose of generalization, the governing equation (2.3.2) will be transformed into dimensionless form. To do this the following dimensionless parameters are introduced:

$$\theta = \frac{T - T_{\infty}}{T_{\infty}}, \quad \zeta = \frac{x}{L}, \quad \eta = \frac{y}{L}, \quad \tau = \frac{t}{t_0}$$

Where t_0 is the term at which t is divided by to have dimensionless time (τ)

and it is equal to $\frac{L^2 \rho C}{k}$.

Substituting these parameters in equation (2.3.2) gives:

$$\frac{\partial \theta}{\partial \tau} = \left[\frac{\partial^2 \theta}{\partial \zeta^2} + \frac{\partial^2 \theta}{\partial \eta^2} \right] - \frac{h_u L^2}{wk} \theta - \frac{h_l L^2}{wk} \theta + \frac{g_0 L^2}{T_{\infty} k} \delta(L\zeta) \delta(L\eta - \bar{V} t_0 \tau) \quad (2.3.3)$$

Let $\beta i = \frac{hL^2}{wk}$, $G_0 = \frac{g_0}{T_\infty k}$ and $V = \frac{\bar{V} t_0}{L}$ and substitute into equation (2.3.3)

gives:

$$\frac{\partial \theta}{\partial \tau} = \left[\frac{\partial^2 \theta}{\partial \zeta^2} + \frac{\partial^2 \theta}{\partial \eta^2} \right] - \beta i_u \theta - \beta i_1 \theta + G_0 \delta(\zeta) \delta(\eta - V\tau) \quad (2.3.4)$$

The dimensionless initial and boundary conditions are:

Initial condition:

$$\theta(0, \zeta, \eta) = 0 \quad (2.3.4a)$$

Boundary conditions:

$$\text{At } \zeta = 0 \quad \frac{\partial \theta}{\partial \zeta} = 0 \quad (2.3.4b)$$

$$\text{At } \zeta = 1 \quad \frac{\partial \theta}{\partial \zeta} = 0 \quad (2.3.4c)$$

$$\text{At } \eta = 0 \quad \frac{\partial \theta}{\partial \eta} = 0 \quad (2.3.4d)$$

$$\text{At } \eta = \frac{H}{L} \quad \frac{\partial \theta}{\partial \eta} = 0 \quad (2.3.4e)$$

Let r be defined as a new term and equal to $\frac{H}{L}$ and be called aspect ratio.

In order to transform (2.3.4) into easier form, the following transformation can be utilized:

Consider an equation of the following form that contains convective and generation terms:

$$\frac{\partial \theta}{\partial \tau} = \alpha \left[\frac{\partial^2 \theta}{\partial \zeta^2} + \frac{\partial^2 \theta}{\partial \eta^2} \right] - \beta_1 \frac{\partial \theta}{\partial \zeta} - \beta_2 \frac{\partial \theta}{\partial \eta} + \gamma \theta + g \quad (2.3.5)$$

Define a new dependent variable $W(\tau, \zeta, \eta)$ such as

$$\theta(\tau, \zeta, \eta) = W(\tau, \zeta, \eta) \cdot \exp \left[\frac{\beta_1}{2\alpha} \zeta - \left(\frac{\beta_1^2}{4\alpha} - \gamma \right) \tau \right] \cdot \exp \left[\frac{\beta_2}{2\alpha} \eta - \frac{\beta_2^2}{4\alpha} \tau \right] \quad (2.3.6)$$

Under this transformation equation (2.3.4) becomes

$$\frac{\partial W}{\partial \tau} = \frac{\partial^2 W}{\partial \zeta^2} + \frac{\partial^2 W}{\partial \eta^2} + G_0 \exp^{-r\tau} \delta(\zeta) \delta(\eta - V\tau) \quad (2.3.7)$$

With the following initial and boundary conditions

Initial conditions:

$$\theta(0, \zeta, \eta) = 0 = W(0, \zeta, \eta) \quad (2.3.7a)$$

Boundary conditions:

$$\text{At } \zeta = 0, l \quad \frac{\partial W}{\partial \zeta} = 0 \quad (2.3.7b)$$

$$\text{At } \zeta = 0, l \quad \frac{\partial W}{\partial \zeta} = 0 \quad (2.3.7c)$$

$$\text{At } \eta = 0, r \quad \frac{\partial W}{\partial \eta} = 0 \quad (2.3.7d)$$

$$\text{At } \eta = 0, r \quad \frac{\partial W}{\partial \eta} = 0 \quad (2.3.7e)$$

Equation (2.3.7) can be solved using Green's function method after finding the homogeneous solution of equation (2.3.7):

Consider the homogenous part of equation (2.3.7):

$$\frac{\partial \psi}{\partial \tau} = \frac{\partial^2 \psi}{\partial \zeta^2} + \frac{\partial^2 \psi}{\partial \eta^2} \quad (2.3.8)$$

Along with initial condition:

$$\psi(0, \zeta, \eta) = 0 = F(\zeta, \eta) \quad (2.3.8a)$$

And boundary conditions:

$$\text{At } \zeta = 0 \quad \frac{\partial \psi}{\partial \zeta} = 0 \quad (2.3.8b)$$

$$\text{At } \zeta = 1 \quad \frac{\partial \psi}{\partial \zeta} = 0 \quad (2.3.8c)$$

$$\text{At } \eta = 0 \quad \frac{\partial \psi}{\partial \eta} = 0 \quad (2.3.8d)$$

$$\text{At } \eta = r \quad \frac{\partial \psi}{\partial \eta} = 0 \quad (2.3.8e)$$

Using separation of variables technique to solve equation (2.3.8) yields

$$\psi(\tau, \zeta, \eta) = \sum_{m=0}^{\infty} \sum_{n=0}^{\infty} e^{-(\beta_m^2 + \epsilon_n^2)\tau} \cdot \frac{1}{N(\beta_m) \cdot N(\epsilon_n)} \cdot \cos(\beta_m \zeta) \cdot \cos(\epsilon_n \eta) \cdot \int_{\zeta'=0}^1 \int_{\eta'=0}^r \cos(\beta_m \zeta') \cdot \cos(\epsilon_n \eta') \cdot F(\zeta, \eta) d\zeta' d\eta' \quad (2.3.9)$$

Where:

$$\frac{1}{N(\beta_m)} = \begin{cases} 2 & \text{for } \beta_m \neq 0 \\ 1 & \text{for } \beta_m = 0 \end{cases}$$

$$\frac{1}{N(\varepsilon_n)} = \begin{cases} \frac{2}{r} & \text{for } \varepsilon_n \neq 0 \\ \frac{1}{r} & \text{for } \varepsilon_n = 0 \end{cases} \quad (2.3.9a)$$

To find the eigenvalues:

$$\sin \beta_m(1) = 0 \quad \Rightarrow \beta_m = m\pi \quad m=0,1,2,\dots \quad (2.3.9b)$$

$$\sin \varepsilon_n(r) = 0 \quad \Rightarrow \varepsilon_n = \frac{n\pi}{r} \quad n=0,1,2,\dots \quad (2.3.9c)$$

In order to find Green's function (G), equation (2.3.9) is rewritten in the following form

$$\psi(\tau, \zeta, \eta) = \int_{\zeta=0}^1 \int_{\eta=0}^r G(\zeta, \eta, \tau | \zeta', \eta', \tau') \Big|_{\tau=0} \cdot F(\zeta', \eta') d\zeta' d\eta' \quad (2.3.10)$$

And so it becomes:

$$\psi = \sum_{m=0}^{\infty} \sum_{n=0}^{\infty} e^{-(\beta_m^2 + \varepsilon_n^2)\tau} \cdot \frac{1}{N(\beta_m) \cdot N(\varepsilon_n)} \cdot \cos \beta_m \zeta \cdot \cos \varepsilon_n \eta \cdot \int_{\zeta=0}^1 \int_{\eta=0}^r F(\zeta', \eta') \cdot \cos \beta_m \zeta' \cdot \cos \varepsilon_n \eta' d\zeta' d\eta' \quad (2.3.11)$$

Finding Green's function:

$$G(\zeta, \eta, \tau | \zeta', \eta', \tau') = \sum_{m=0}^{\infty} \sum_{n=0}^{\infty} e^{-(\beta_m^2 + \varepsilon_n^2)(\tau - \tau')} \cdot \frac{1}{N(\beta_m) \cdot N(\varepsilon_n)} \cdot \cos \beta_m \zeta \cdot \cos \varepsilon_n \eta \cdot \cos \beta_m \zeta' \cdot \cos \varepsilon_n \eta' \quad (2.3.12)$$

Now to solve (2.3.8), we substitute in the following equation:

$$\begin{aligned}
 W(\zeta, \eta, \tau) = & \int_A G(r, \tau | r', \tau') \Big|_{\tau'=0} \cdot F(\zeta, \eta) d\zeta' d\eta' + \int_{\tau'=0}^{\tau} \int_A G(r, \tau | r', \tau') \cdot g(r', \tau') dA' \\
 & + \int_{\tau'=0}^{\tau} d\tau' \sum_{i=1}^{\infty} \int_{\substack{\text{boundary A} \\ \text{bath}}} \int G(r, \tau | r', \tau') \Big|_{r'=r_i} \frac{f_i}{k_i} dl_i
 \end{aligned}
 \tag{2.3.13}$$

However,

$$\int_{\tau'=0}^{\tau} d\tau' \sum_{i=1}^{\infty} \int_{\substack{\text{boundary A} \\ \text{bath}}} \int G(r, \tau | r', \tau') \Big|_{r'=r_i} \frac{f_i}{k_i} dl_i = 0
 \tag{2.3.14}$$

Which upon substituting in equation (2.3.13), yields:

$$\begin{aligned}
 W(\zeta, \eta, \tau) = & \int_{\zeta'=0}^1 \int_{\eta'=0}^1 \sum_{m=0}^{\infty} \sum_{n=0}^{\infty} e^{-(\beta_m^2 + \epsilon_n^2)\tau} \cdot \frac{1}{N(\beta_m) \cdot N(\epsilon_n)} \cdot \cos \beta_m \zeta' \cdot \cos \epsilon_n \eta' \\
 & \cdot \cos \beta_m \zeta' \cdot \cos \epsilon_n \eta' \cdot F(\zeta, \eta) d\zeta' d\eta' \\
 & + \int_{\tau'=0}^{\tau} d\tau' \int_{\zeta'=0}^1 \int_{\eta'=0}^1 \sum_{m=0}^{\infty} \sum_{n=0}^{\infty} e^{-(\beta_m^2 + \epsilon_n^2)\chi(\tau-\tau')} \frac{1}{N(\beta_m) \cdot N(\epsilon_n)} \cdot \cos \beta_m \zeta' \cdot \cos \epsilon_n \eta' \\
 & \cdot \cos \beta_m \zeta' \cdot \cos \epsilon_n \eta' \cdot G_0 e^{-\pi'} \delta(\zeta') \delta(\eta' - V\tau') d\zeta' d\eta'
 \end{aligned}
 \tag{2.3.15}$$

Also:

$$\int_{\zeta'=0}^1 \cos(\beta_m \zeta') \delta(\zeta') d\zeta' = 1
 \tag{2.3.16}$$

And

$$\int_{\eta'=0}^1 \cos(\epsilon_n \eta') \delta(\eta' - V\tau') d\eta' = \cos(\epsilon_n V\tau')
 \tag{2.3.17}$$

The first term in equation (2.3.15) cancels since $F(\zeta, \eta) = 0$

Substituting (2.3.16) and (2.3.17) into (2.3.15) gives:

$$W(\zeta, \eta, \tau) = \int_{\tau^*=0}^{\tau} \sum_{m=0}^{\infty} \sum_{n=0}^{\infty} e^{-(\beta_m^2 + \varepsilon_n^2) \chi_{\tau-\tau^*}} \frac{1}{N(\beta_m) \cdot N(\varepsilon_n)} \cdot \cos(\beta_m \zeta) \cdot \cos(\varepsilon_n \eta) \cdot \cos(\varepsilon_n V \tau^*) \cdot G_0 e^{-\gamma \tau^*} d\tau^* \quad (2.3.18)$$

Combining similar-time-terms:

$$W(\zeta, \eta, \tau) = \int_{\tau^*=0}^{\tau} \sum_{m=0}^{\infty} \sum_{n=0}^{\infty} e^{-(\beta_m^2 + \varepsilon_n^2) \tau} \frac{1}{N(\beta_m) \cdot N(\varepsilon_n)} \cdot \cos(\beta_m \zeta) \cdot \cos(\varepsilon_n \eta) \cdot \cos(\varepsilon_n V \tau^*) \cdot G_0 e^{(\beta_m^2 + \varepsilon_n^2 - \gamma) \tau^*} d\tau^* \quad (2.3.19)$$

Rearranging:

$$W(\zeta, \eta, \tau) = \sum_{m=0}^{\infty} \sum_{n=0}^{\infty} e^{-(\beta_m^2 + \varepsilon_n^2) \tau} \frac{\cos(\beta_m \zeta) \cdot \cos(\varepsilon_n \eta)}{N(\beta_m) \cdot N(\varepsilon_n)} \cdot \int_{\tau^*=0}^{\tau} G_0 \cdot \cos(\varepsilon_n V \tau^*) e^{(\beta_m^2 + \varepsilon_n^2 - \gamma) \tau^*} d\tau^* \quad (2.3.20)$$

Integrating by parts:

$$\int_{\tau^*=0}^{\tau} G_0 \cdot \cos(\varepsilon_n V \tau^*) e^{(\beta_m^2 + \varepsilon_n^2 - \gamma) \tau^*} d\tau^* = \frac{G_0}{(\beta_m^2 + \varepsilon_n^2 - \gamma)^2 + \varepsilon_n^2 V^2} \{ \varepsilon_n V e^{(\beta_m^2 + \varepsilon_n^2 - \gamma) \tau} \cdot \sin(\varepsilon_n V \tau) + (\beta_m^2 + \varepsilon_n^2 - \gamma) \cdot e^{(\beta_m^2 + \varepsilon_n^2 - \gamma) \tau} \cdot \cos(\varepsilon_n V \tau) - (\beta_m^2 + \varepsilon_n^2 - \gamma) \} \quad (2.3.21)$$

Substituting (2.3.21) into (2.3.20), results in:

$$W(\zeta, \eta, \tau) = \sum_{m=0}^{\infty} \sum_{n=0}^{\infty} e^{-(\beta_m^2 + \varepsilon_n^2) \tau} \frac{\cos(\beta_m \zeta) \cdot \cos(\varepsilon_n \eta)}{N(\beta_m) \cdot N(\varepsilon_n)} \cdot \frac{G_0}{(\beta_m^2 + \varepsilon_n^2 - \gamma)^2 + \varepsilon_n^2 V^2} \{ \varepsilon_n V e^{(\beta_m^2 + \varepsilon_n^2 - \gamma) \tau} \cdot \sin(\varepsilon_n V \tau) + (\beta_m^2 + \varepsilon_n^2 - \gamma) \cdot e^{(\beta_m^2 + \varepsilon_n^2 - \gamma) \tau} \cdot \cos(\varepsilon_n V \tau) - (\beta_m^2 + \varepsilon_n^2 - \gamma) \} \quad (2.3.22)$$

From the transformation used previously, it was found that $(\theta = We^{\tau})$ and accordingly equation (2.3.21) becomes:

$$\theta(\zeta, \eta, \tau) = \sum_{m=0}^{\infty} \sum_{n=0}^{\infty} e^{-(\beta_m^2 + \epsilon_n^2 - \gamma)\tau} \frac{\cos \beta_m \zeta \cdot \cos \epsilon_n \eta}{N(\beta_m) \cdot N(\epsilon_n)} \cdot \frac{G_0}{(\beta_m^2 + \epsilon_n^2 - \gamma)^2 + \epsilon_n^2 V^2} \cdot \{ \epsilon_n V e^{(\beta_m^2 + \epsilon_n^2 - \gamma)\tau} \cdot \sin(\epsilon_n V \tau) + (\beta_m^2 + \epsilon_n^2 - \gamma) \cdot e^{(\beta_m^2 + \epsilon_n^2 - \gamma)\tau} \cdot \cos(\epsilon_n V \tau) - (\beta_m^2 + \epsilon_n^2 - \gamma) \} \quad (2.3.23)$$

After extracting common term, the final solution is:

$$\theta(\zeta, \eta, \tau) = \sum_{m=0}^{\infty} \sum_{n=0}^{\infty} \frac{\cos \beta_m \zeta \cdot \cos \epsilon_n \eta}{N(\beta_m) \cdot N(\epsilon_n)} \cdot \frac{G_0}{(\beta_m^2 + \epsilon_n^2 - \gamma)^2 + \epsilon_n^2 V^2} \cdot \{ \epsilon_n V \cdot \sin(\epsilon_n V \tau) + (\beta_m^2 + \epsilon_n^2 - \gamma) \cdot \cos(\epsilon_n V \tau) - (\beta_m^2 + \epsilon_n^2 - \gamma) e^{-(\beta_m^2 + \epsilon_n^2 - \gamma)\tau} \} \quad (2.3.24)$$

Equation (2.3.24) gives the dimensionless temperature distribution at any location specified on the plate. Since equation (2.3.24) will be used in the following chapters it was programmed using Fortran 77 and its codes are shown in appendix A.

CHAPTER THREE

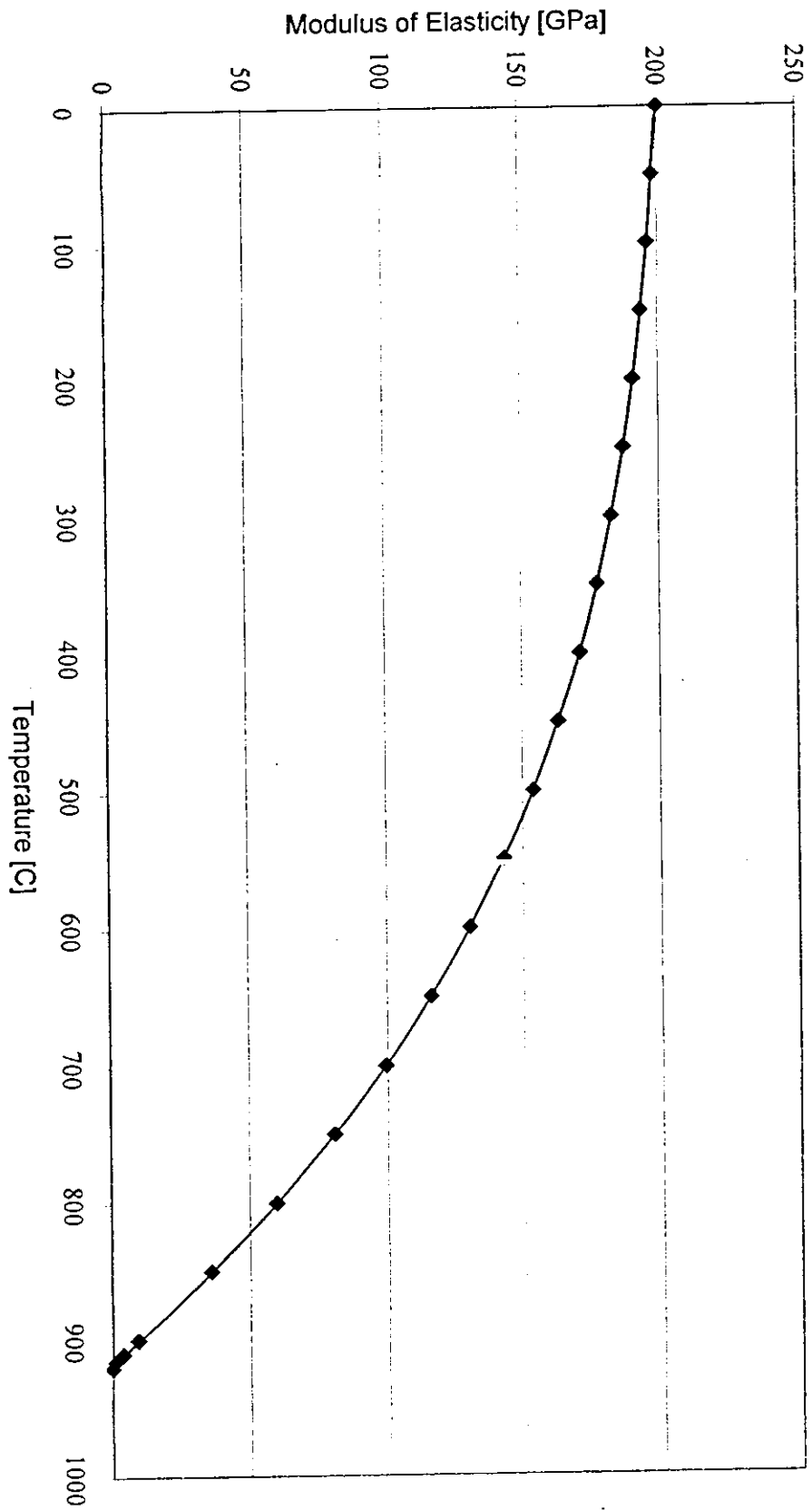
DETERMINATION OF THERMAL AND RESIDUAL STRESSES

3.1 Introduction

In the previous chapter, the temperature distribution within the plate during the welding process was determined. So now it is possible to find the temperature at any certain location at any certain moment. Temperature distribution determination is the most important step necessary for computation of thermal and residual stresses.

3.2 Physical Properties

The Yield strength (σ), Young's Modulus of elasticity (E) and Coefficient of thermal expansion (α), are needed for the calculation of thermal stresses. These properties are temperature dependent and vary considerably at elevated temperatures. One of the important steps in the evaluation of thermal and residual stresses is the determination of these quantities at each temperature. Figures (3.2.1) through (3.2.3) show the approximate variation of these three physical properties with temperature for mild steel (Tall, 1964). The word "approximate" is used here since the measurements of these values at elevated temperature is very difficult and there is great variation in the values of these properties obtained by different investigators.



Figure(3.2.1) Modulus of Elasticity for mild steel (Tall, 1964)

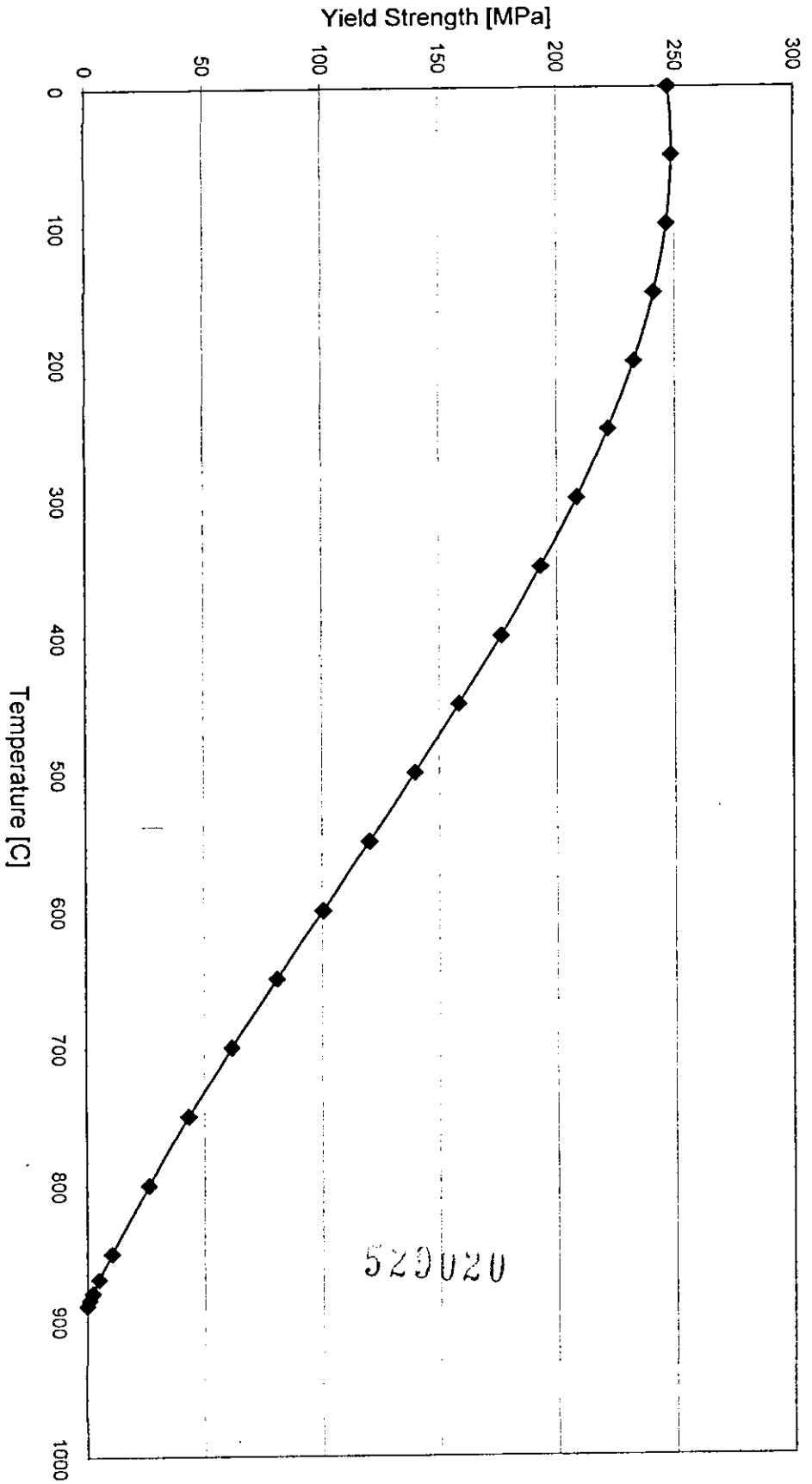


Figure (3.2.2) Yield stress for mild steel (Tall, 1964)

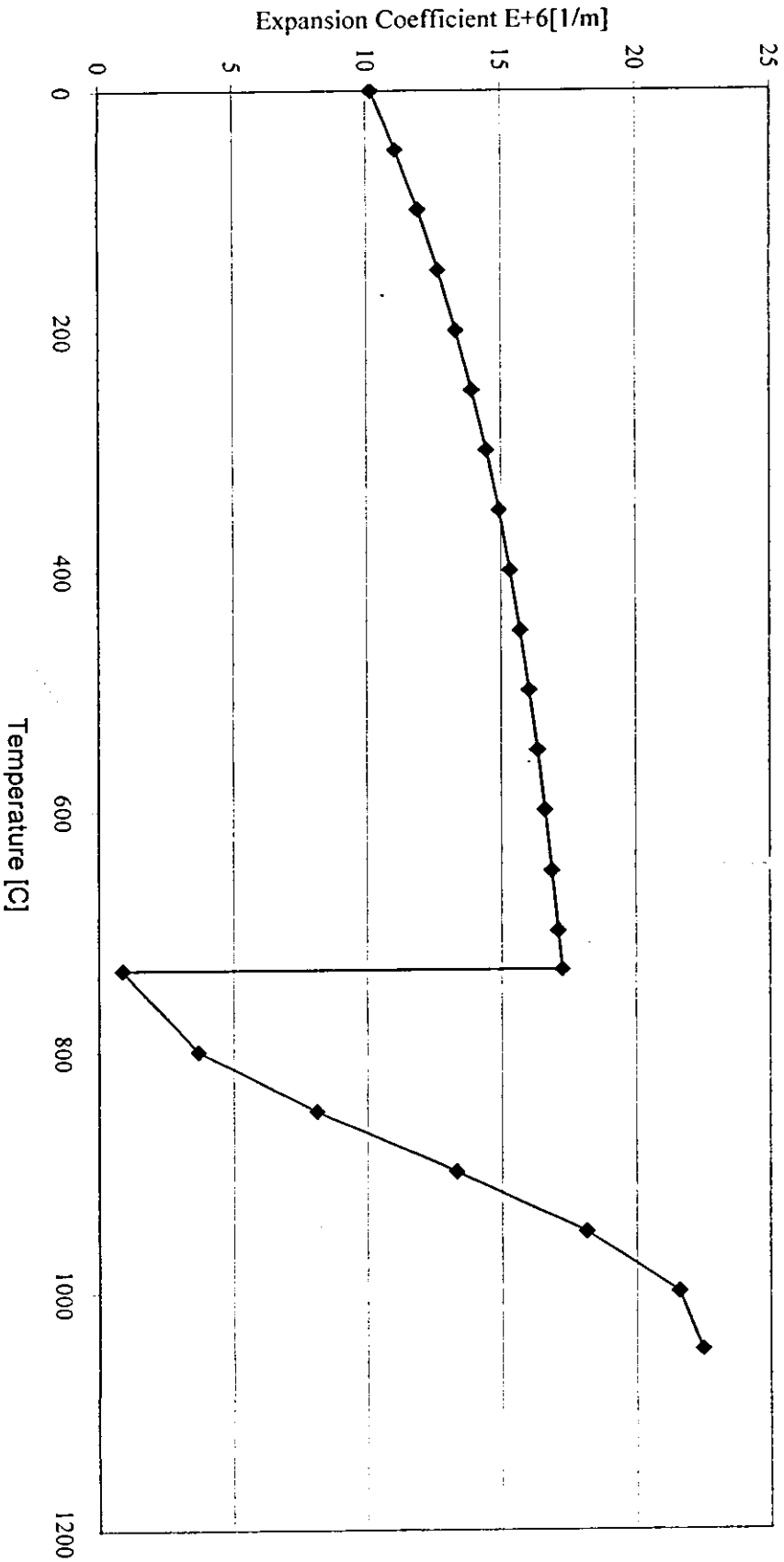


Figure (3.2.3) Coefficient of Liner Thermal Expansion for mild steel (Tall, 1964)

Since Figures (3.2.1,2 and 3) are so important for computing thermal stresses, they are fitted using certain computer software that gives best-fit polynomials. The figures show both data points as discrete points and the fitting polynomials. The obtained polynomials are programmed using Fortran 77 and it is shown in appendix B.

3.3 Thermal Stresses

Stresses owing to the restriction of thermally induced expansion or contraction of a body are termed thermal stresses (Ugural 1980). Produced thermal stresses during welding can be well understood from the following discussion:

Figure (3.3.1) shows the typical temperature variations and the resulting thermal stresses inside a welded plate at different stages (Masubuchi, 1980). The figure also shows the arc travelling with a speed of (v) . The line behind the arc represents a just-welded area.

Along section A-A, which represents area ahead of the arc, the temperature variation due to welding is zero and the resulting produced thermal stress is consequently zero.

Along section B-B, which crosses the currently welded point, the temperature variation due to welding is very sharp. High temperature exceeds the melting temperature exists near the weld line and it decreases as moving away along the section. Stresses close to welding arc are zero

because molten metal does not support loads. Stresses far a little from the weld line are compressive because the expansion of these areas is restricted by lower temperature metal. Stresses in areas far away from the weld line are tensile and balance with compressive stresses. One should note that due to the temperature, the stresses close to weld line are as high as the yield strength at that temperature.

Along section C-C, which represents a region behind the arc, temperature variation due to welding is less sharp than section B-B because weld metal and base metal have cooled down. Therefore this cooling makes both metals try to shrink causing tensile stresses close to the weld. As the distance is increasing along the same section, the stress becomes compressive and then changes to tensile.

Very far from the arc torch and along section D-D, the temperature variation is almost zero. However, high stresses close to the weld are produced while compressive stresses are produced as a result of balance condition.

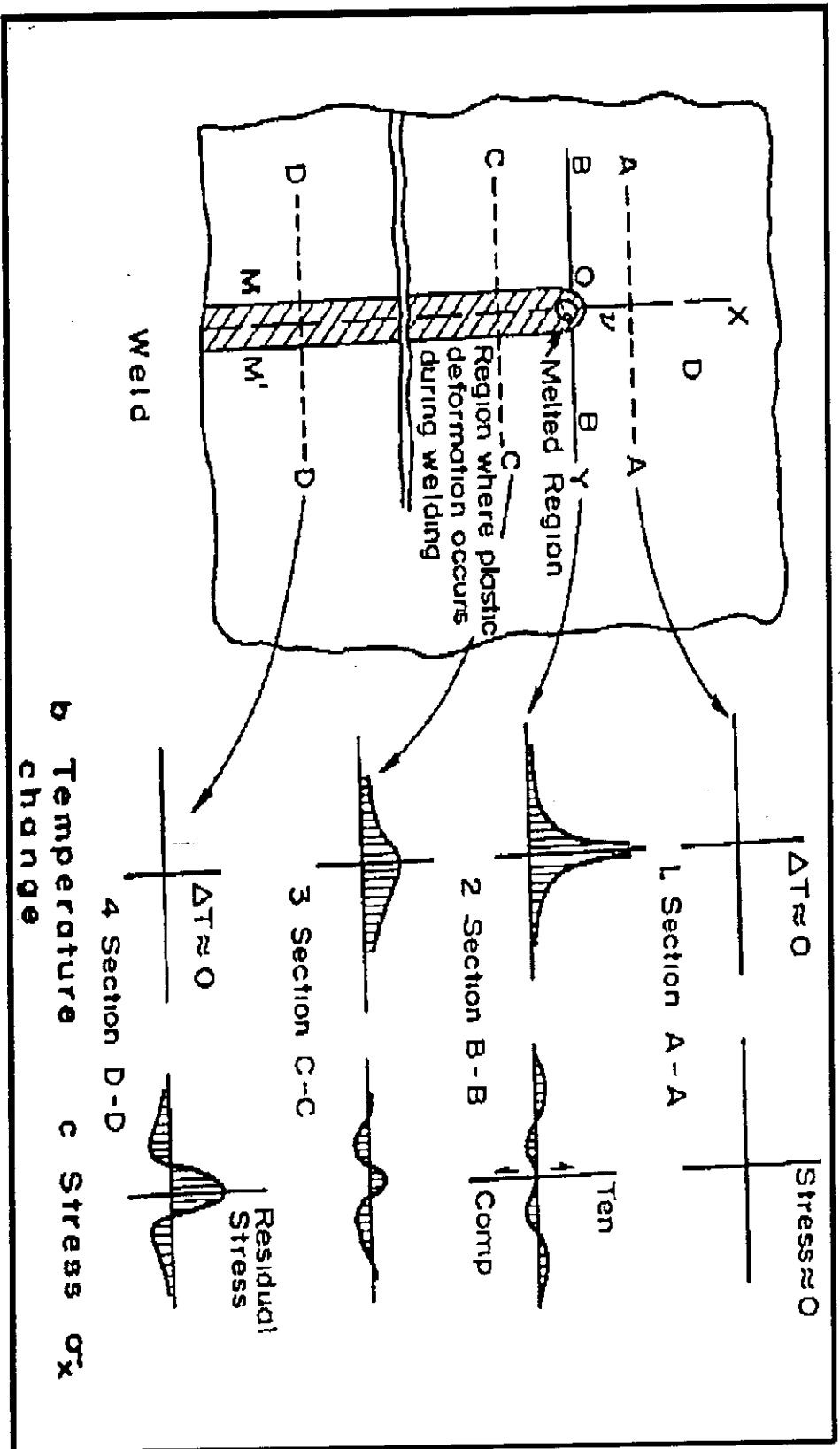


Figure (3.3.1) Schematic representation of changes of temperature and stresses during welding (Masubuchi, 1980)

Computation of Thermal Stress

The total strains at each point of a heated body compose of two parts. The first one is uniform expansion proportional to the temperature rise ΔT . The second one is due to stress resulting from external forces.

In the present work, the material (mild steel) is assumed to be homogenous and isotropic with no external forces acting on the plate. It is also assumed that the stress variations in the y direction are much less than those in the x direction. Based on this, the thermal stress due to temperature rise can be calculated as in the following equation

$$\sigma_{\text{thermal}} = E\alpha\Delta T \quad (3.3.1)$$

The value of the thermal stress σ_{thermal} is limited by the yield stress at that temperature. The values of the physical properties E and α can be determined from figure (3.2.1) and figure (3.2.3).

3.4 Residual Stress

Residual stresses are those stresses that would exist in a body if all external loads were removed (Masubuchi, 1980). Residual stresses exist on both microscopic scale such as the stress which exist in areas near dislocation, and on macroscopic scale, such as those occurring in plate after welding process or that occurs in a bar during rolling process.

Equilibrium condition of residual stresses

From the definition of residual stresses, the resultant force and the resultant moment must equal zero. In equation form, the force equilibrium requires that

$$\int \sigma \cdot dA = 0 \quad (3.4.1)$$

and the moment equilibrium requires that:

$$\int dM = 0 \quad (3.4.2)$$

where A is the area and M is moment.

The above conditions must apply in any calculation of residual stress.

As seen from figure (3.3.1), residual stresses are the stresses that remain after the thermal cycle is completed and reaches the yield stress at room temperature. Post-weld heat-treatment is often used to lower the magnitude of residual stress (Olabi and Hashmi, 1996).

3.5 Computation of Thermal and Residual Stresses

In the present work, a numerical procedure based on the method presented originally by Tall (1964) is used to compute the thermal and residual stresses. In this procedure the temperature distribution is calculated, then the thermal stresses corresponding to temperature increments are computed and added to the previous computed thermal stresses limited by the yield stresses at that temperature. The summation of forces produced in the plate due to these thermal stresses along a certain section must equal zero to

fulfill the equilibrium condition. The stresses accumulated in the plate after cooling are the residual stresses.

The following is a step by step procedure for computation of thermal and residual stresses. Since the greatest changes in temperature occur immediately after the onset of welding, the time increment to be used in the calculations should be short at the beginning. Starting with zero time, the thermal stress is calculated for the initial temperature using equation (3.3.1). The temperature at the next time increment is also determined using equation (2.3.23). The average temperature between the two consequent time interval is calculated. The values of coefficient of linear expansion, Modulus of elasticity and the yield stress are taken from figure (3.2.1) to figure (3.2.3). The thermal stress corresponding to this temperature increment is calculated using equation (3.3.1). This value is added to the thermal stress in the previous time and is being limited as a maximum by the yield stress at that temperature. For the purpose of applying the equilibrium condition the width of the plate is divided into strips, narrower strips near the weld and wider as moving away from the weld along that transverse section. To find the forces produced inside the thin plate due to this thermal stress, the calculated thermal stress is multiplied by the area of the strip. If the summation of forces along the cross section is close or equal to zero, then the equilibrium condition applies. Since the present case is center welding one, no moment

equilibrium will be taken into account (since this is already satisfied). If the summation of these forces is not close or equal zero, a new term is introduced to the thermal stress, which is the equilibrium stress σ_{equ} . Since the actual thermal stress for the time increment is a summation of the temperature stress σ_{thermal} and equilibrium stress σ_{equ} and since this summation is actually simultaneous, a trial and error method must be used in the computation process. The initial value of σ_{equ} is chosen arbitrary and added to σ_{thermal} and the summation is limited by the value of the yield stress at each corresponding temperature. The new produced forces inside the thin plate are calculated by multiplying the stresses by the area of the strips again. The value of σ_{equ} is changed (either increased or decreased) until the summation of forces is close to or equal to zero. Now the stress distribution inside the thin plate at that instant is determined. The algebraic equation which describes the above procedure, is

$$(\sigma_{\text{thermal}})_t = (\sigma_{\text{thermal}})_{t-1} + E\alpha\Delta T + \sigma_{\text{equ}} \quad (3.5.1)$$

where t is time instant.

The above procedure is repeated for each time interval until last, the thermal stresses at the last step being that at the cooled temperature is that the residual stress. The above procedure is programmed using Fortran language (see appendix C+D).

It should be noted that the major step in this computational method is adding together the incremental thermal stresses; the previous thermal stress and equilibrium stress. In reality the stress formation is simultaneous with that of equilibrium stress, but the addition is a computational approach to find the formed stresses inside the plate.

CHAPTER FOUR

RESULTS AND DISCUSSION

4.1 Introduction

In chapter two, the boundary value problem was solved and a closed form solution for the temperature distribution inside the plate at different times was found. This closed form solution was programmed using Fortran 77 language (see appendices A). Chapter three presented an overview how the thermal and residual stresses are formed and how they are calculated within a thin plate. This procedure was also programmed using Fortran 77 language (see appendices C and D). Now the necessary information determined in the previous chapters will be used to study the effects of changing many welding parameters on the temperature distribution and residual stresses produced in the thin plate during welding process.

4.2 Numerical Data

The residual stress is to be determined in a thin mild steel plate (see figure (2.1.1)) with the following specifications:

Material: Mild steel with the following properties

Mass density (ρ): 7800 kg/m³

Specific heat (C): 450 J/kg. C^o

Thermal conductivity (K) =65W/m.C^o

Plate width (H) = 1.5m

Plate length (L) = 0.3m

Plate thickness (w) = 0.005m

Velocity of welding electrode = 0.003m/s

Plate initial temperature (T_{∞}) = 300K°

Convective heat transfer coefficient (from steel to air) = 15 W/m². K

Heat source intensity (G_0) = 6.5

Heat source intensity is chosen large enough to ensure melting of parent material and reaching reasonable temperature.

The current position of the welding heat source is at $\zeta=0.0$, $\eta=0.4$

The above specified plate dimensions and parameters are used in most cases, but some of them are changed once a time in the following results to investigate their effect on the thermal and residual stresses, each changing is mentioned in its place as will be seen later.

Determination of the dimensionless parameters used in the derivation and required for the computer programs:

$$t_0 = \frac{L^2 \rho C}{K} = \frac{0.3^2 * 7800 * 450}{65} = 4860$$

$$V = \frac{\bar{V} * t_0}{L} = \frac{.003 * 4860}{0.3} = 48.6$$

$$\beta i = \frac{h * L^2}{W * K} = \frac{15 * 0.3^2}{.005 * 65} = 4.153846154$$

$$\gamma = -(\beta i_t + \beta i_u) = -(4.153846154 + 4.153846154) = -8.307692308$$

$$\tau = \frac{t}{t_o} = \frac{1.5/0.003}{4860} = 0.10288$$

The plate is assumed to be vertical oriented during welding process (vertical welding)

4.3 RESULTS AND DISCUSSION

The calculations start on a strip some distance ahead of the arc where the temperature change is negligible and the stresses are purely elastic. Time zero is fixed on the strip, the heat source is assumed arbitrarily to be located at about 12 cm ($\eta=0.4$) ahead of the arc.

Figure (4.3.1) shows the dimensionless temperature changes along the weld centerline $\zeta=0.0$, $\zeta=0.167$, $\zeta=0.333$ and $\zeta=1$. The abscissa is given in terms of dimensionless time. Each curve shows the thermal cycle at a point some distance away from the weld. It is clear from the figure that very high temperature is reached at the centerline of the weld while a small increase in temperature takes place very far from weld line. A sudden increase in

temperature is noticed due to the assumption that the heat source location is specified by unit step function.

Figure (4.3.2) shows stress changes along $\zeta=0.0$, $\zeta=0.167$, $\zeta=0.33$ and $\zeta=1$. Along the weld centerline $\zeta=0.0$, stresses are in compression in areas ahead of the heat source. As the temperature increases, the absolute value of the compressive stress first increases and then decreases. At the point, directly below the heat source, the stresses are zero. This is due to the fact that the material is molten and can resist no load. After the moving of the arc, the area cools down, and the stresses become tensile and reach the yield level at the corresponding temperature.

Figure (4.3.3) shows the residual stress distribution inside the plate. The figure shows that the area close to the weld line carries a tensile residual stress and its value reaches the yield level at room temperature. As moving away from the weld line along the same transverse section, the stress decreases and becomes compressive to account for equilibrium.

The temperature changes (thermal cycles) at different longitudinal lines ($\zeta=0.0$ and $\eta=0.0, 0.4, 0.8, 1.2$ and 1.6) are shown in figure (4.3.4). From the figure the same thermal cycle is repeated but shifted except at $\zeta=0$ where different behavior was noticed, (the high temperature reached is

comparatively low). This explains considering a section far a little from the edge which is arbitrary taken $\eta=0.4$ and used in the most cases during analysis.

The heat source intensity was varied to study its effect on thermal cycles and residual stresses. Figure (4.3.5) shows the thermal cycles for different values of heat input namely for $G_o=2, 4, 6.5$ and 9. The same thermal cycles in shape were obtained but different in the values of the cycle. It is found that as the value of heat intensity increases, higher temperature distribution is obtained due to the fact that this causes more heat to be deposited to the plate. The effects of these changes on residual stress distribution are shown in figure (4.3.6). From the figure, it is clear that the width of the tensile residual zone increases as the value of input heat is increased. The heat input is considered as the most significant factor affecting the width of the tensile stress zone (Masubuchi 1980). From practical viewpoint, the results clearly show the advantage of using a low welding heat input to reduce residual stresses.

Figure (4.3.7) shows the effect of changing weld speed on thermal cycles. Four welding speeds were taken into consideration, namely in dimensional values ($\bar{V}=1, 3, 5$ and 9 mm/sec). From the figure, it is clear that as weld speed decreases, higher temperature values are reached inside the plate.

This is due to the fact that more power is being delivered to the plate per unit time, also longer time to finish welding is needed because the welding speed process is slow.

Figure (4.3.8) shows the effect of changing weld speeds on the residual stress distribution inside the plate. It is depicted that as weld speed decreases, the width of the tensile residual stress zone increases. This is referred to the fact that slower weld speed leads to an increase in the input heat deposited to the plate.

The thickness of the plate was considered, three thicknesses were taken into consideration $w=5,8$ and 15 mm. It is worth mentioning here that the plate is still considered thin. The effect of this change on the thermal cycle is shown in figure (4.3.9).

Figure (4.3.9) shows that the thermal cycles almost coincide, which means that, negligible effect on thermal cycles is noticed due to this change of the thicknesses. Slight effect on the residual stress distribution is also noticed in figure (4.3.10) due to the variation of the plate thickness.

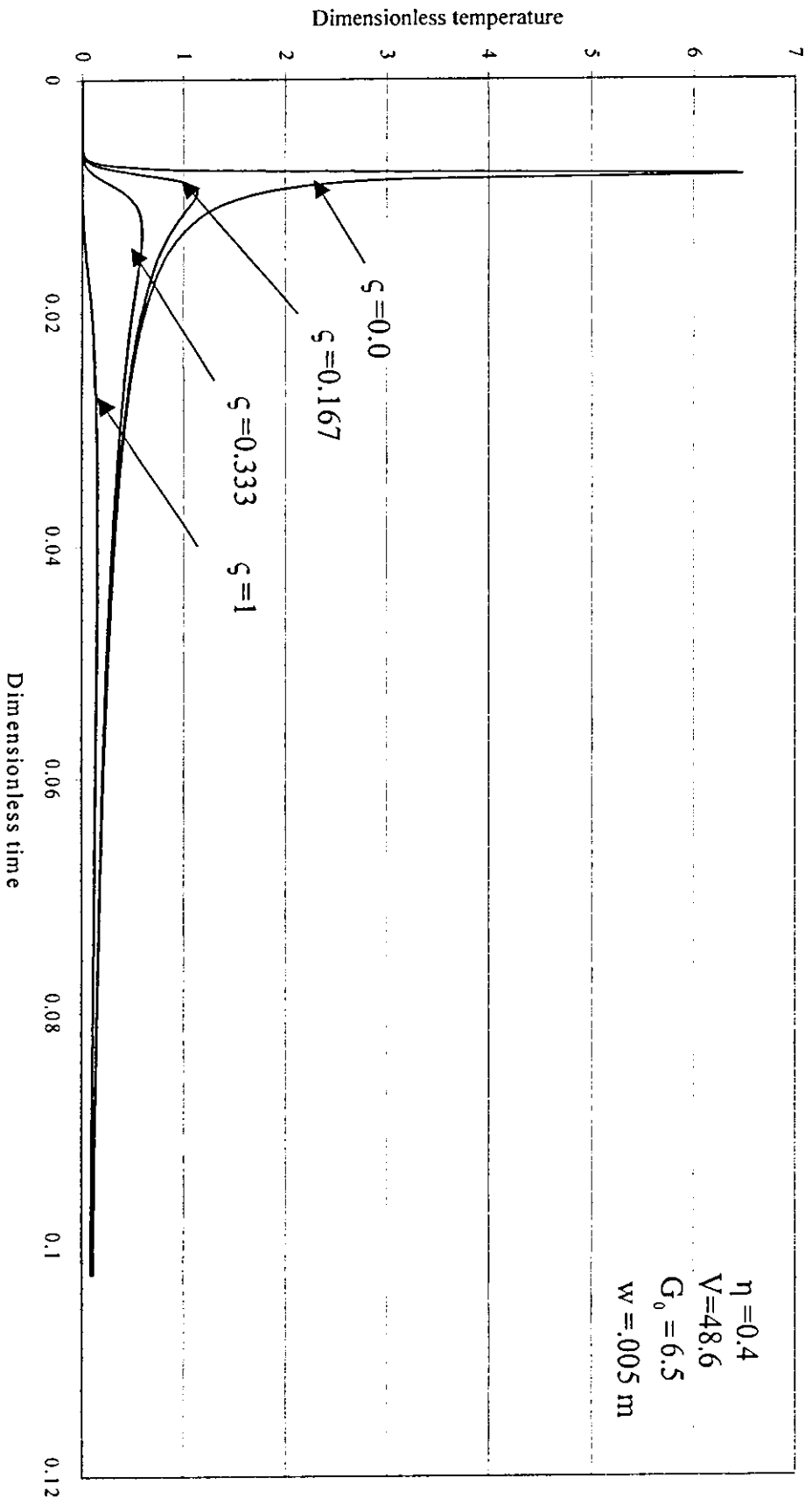


Figure (4.3.1) Temperature changes at different longitudinal lines

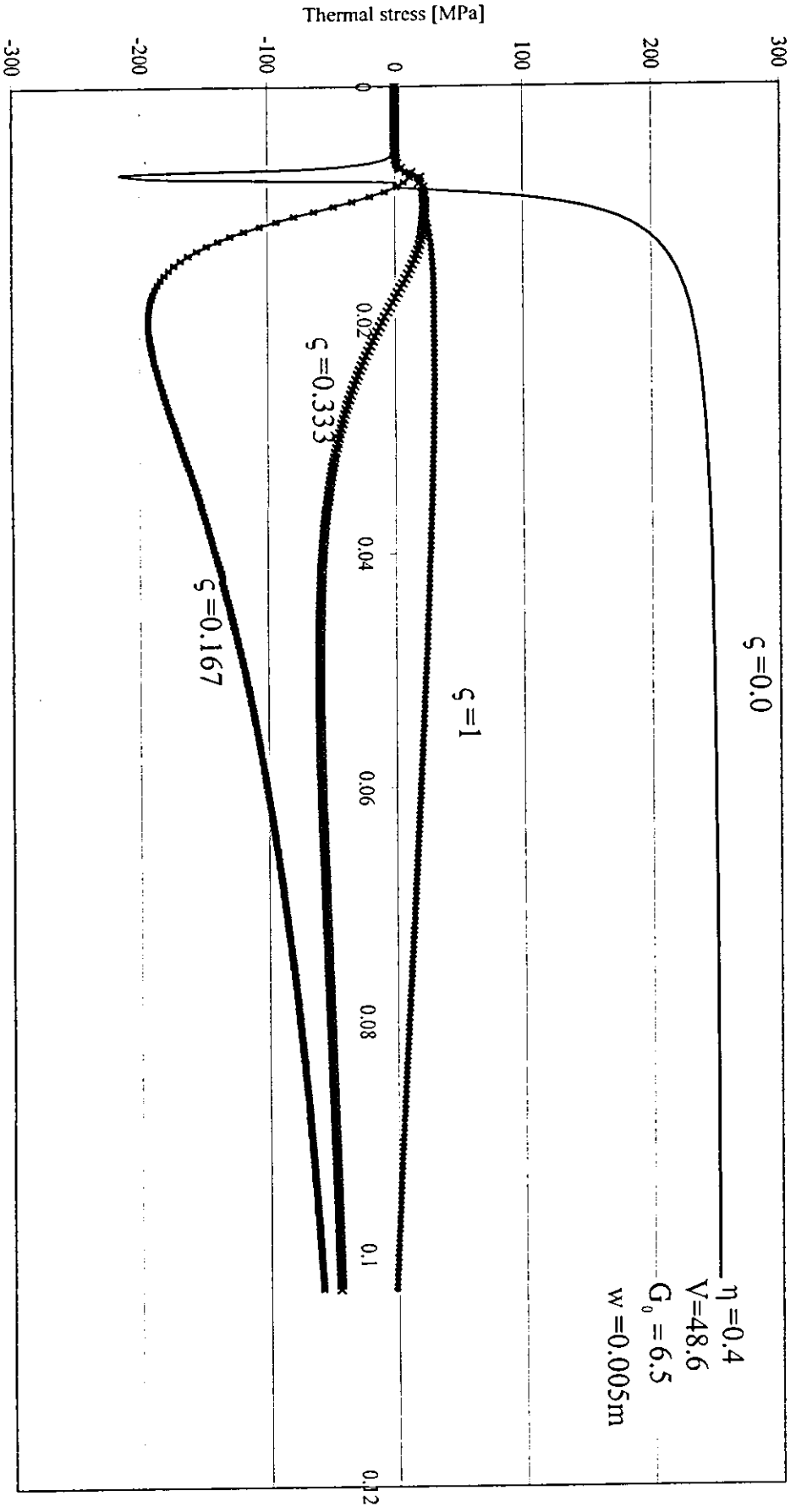
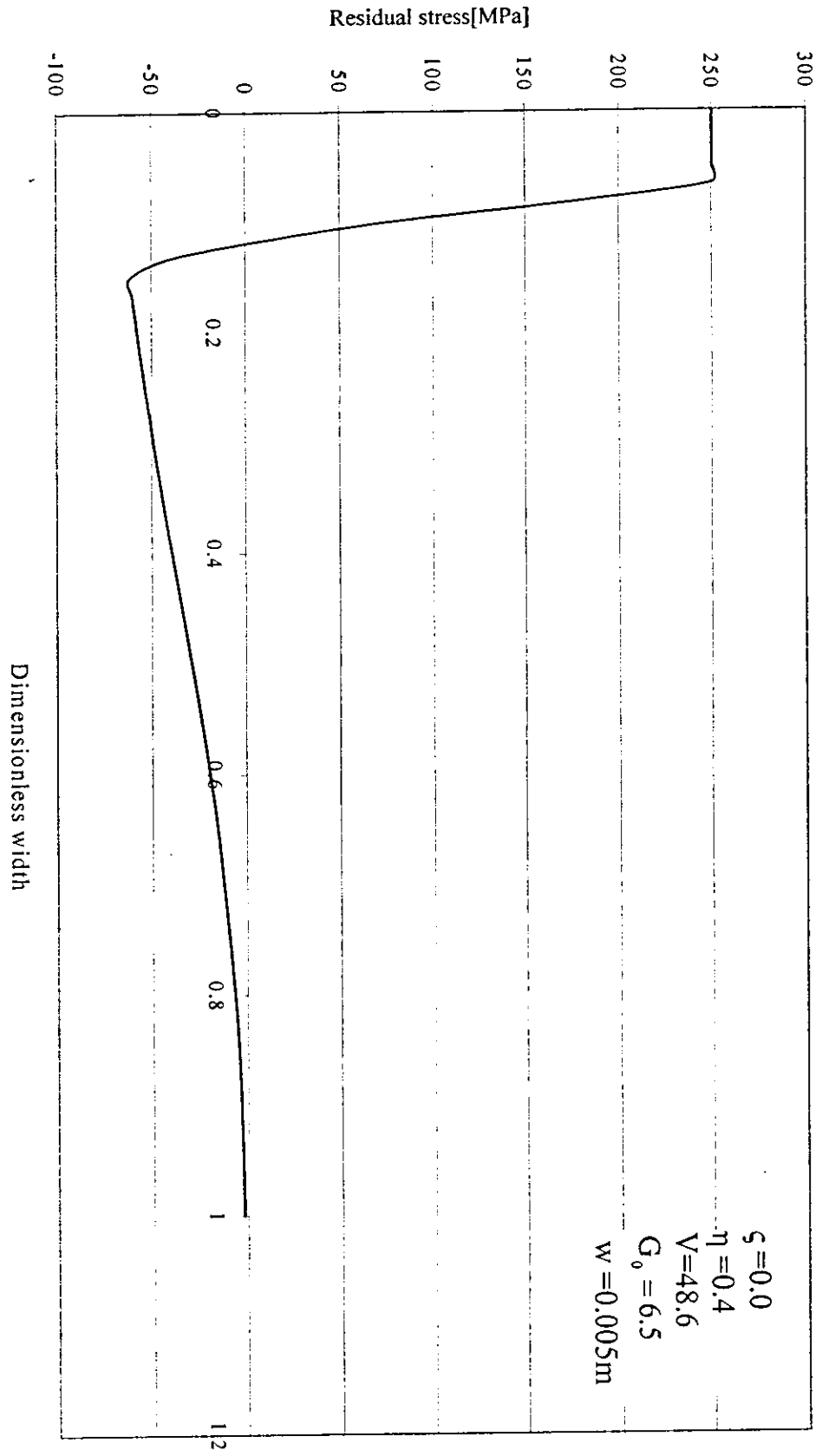


Figure (4.3.2) Stress changes at different longitudinal lines



Figure(4.3.3) Residual Stress distribution inside the plate

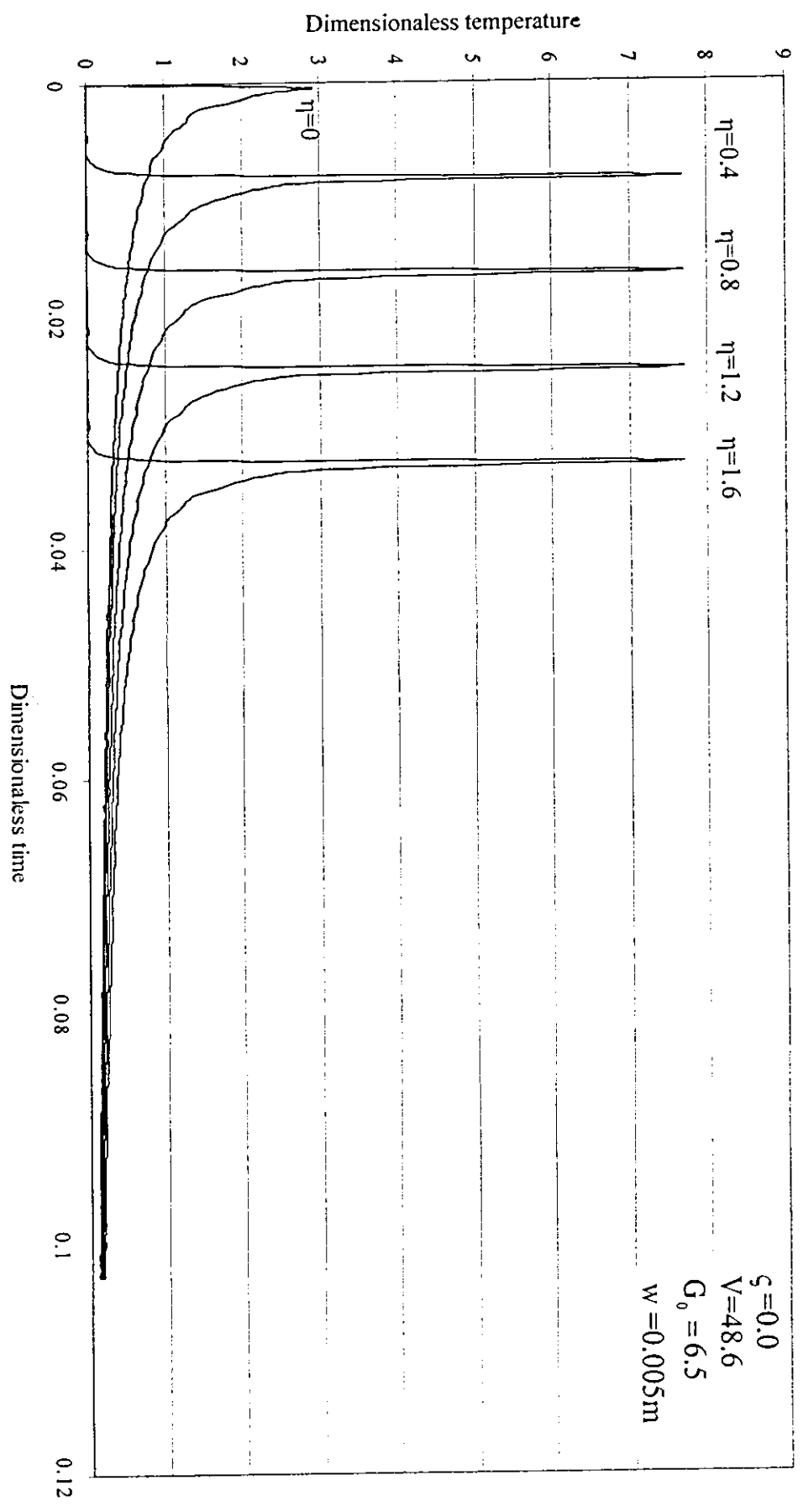
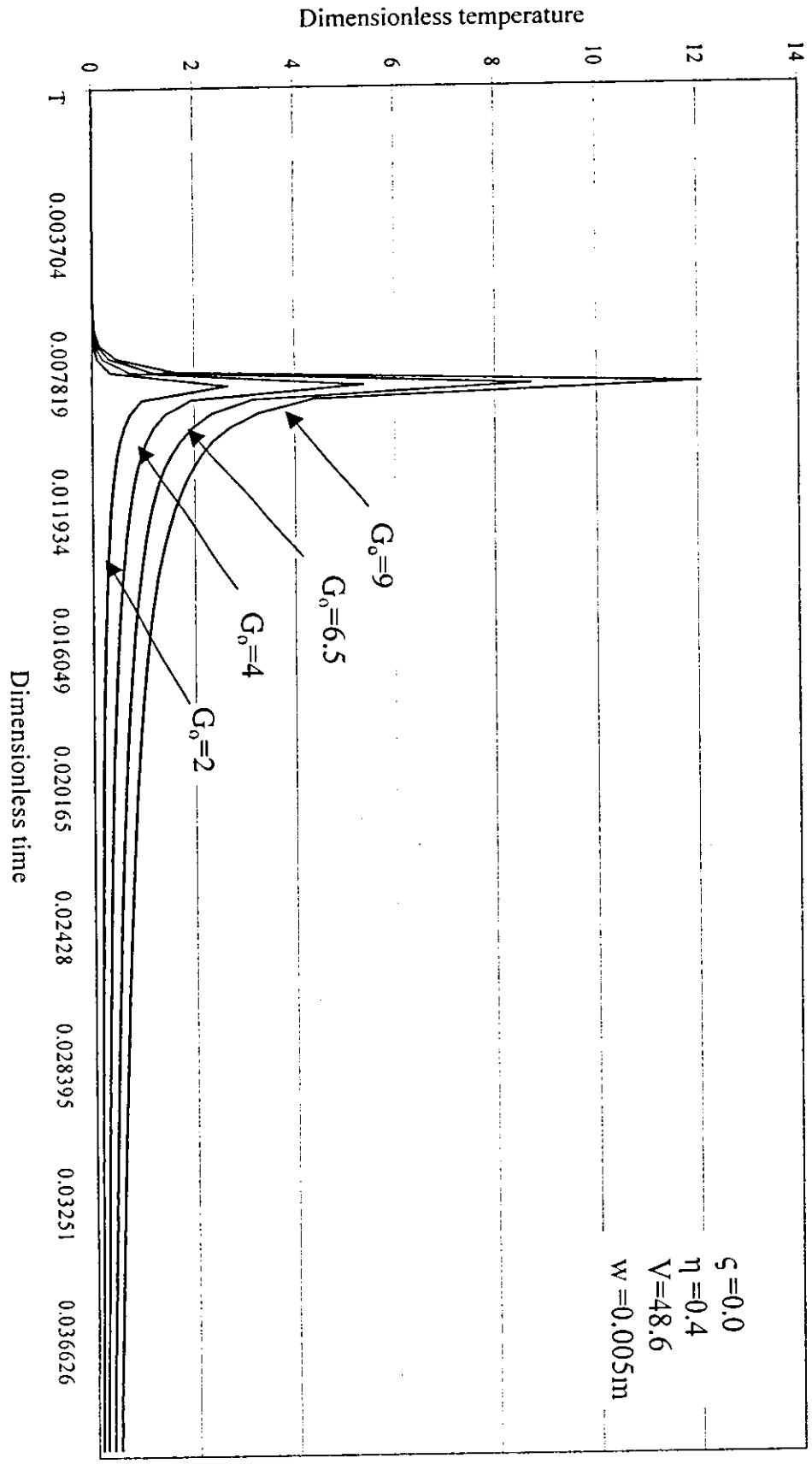


Figure (4.3.4) Thermal cycles at different transverse lines



Figure(4.3.5) Temperature changes at different input heat intensities

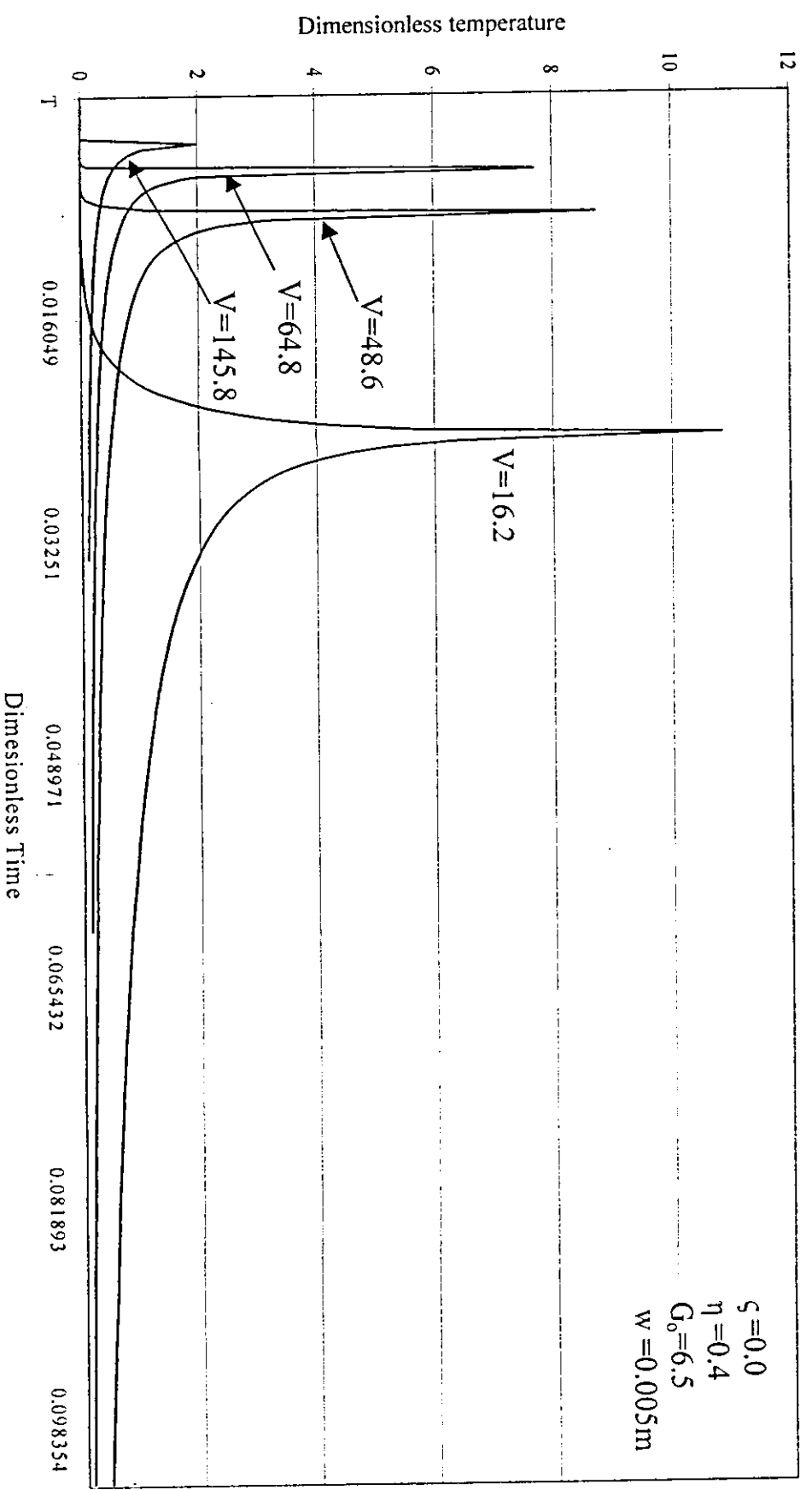


Figure (4.3.7) Temperature changes at different weld speeds

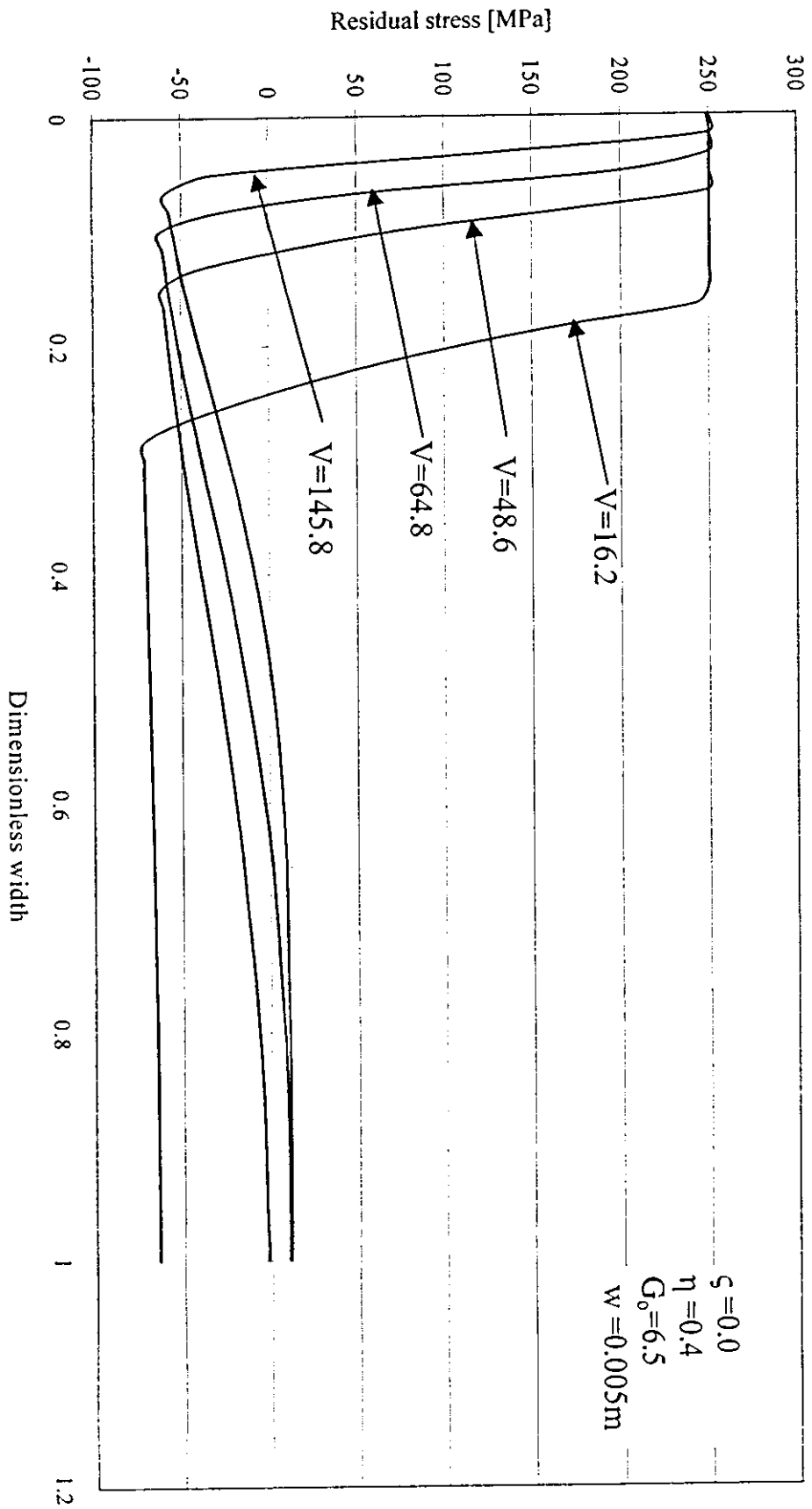
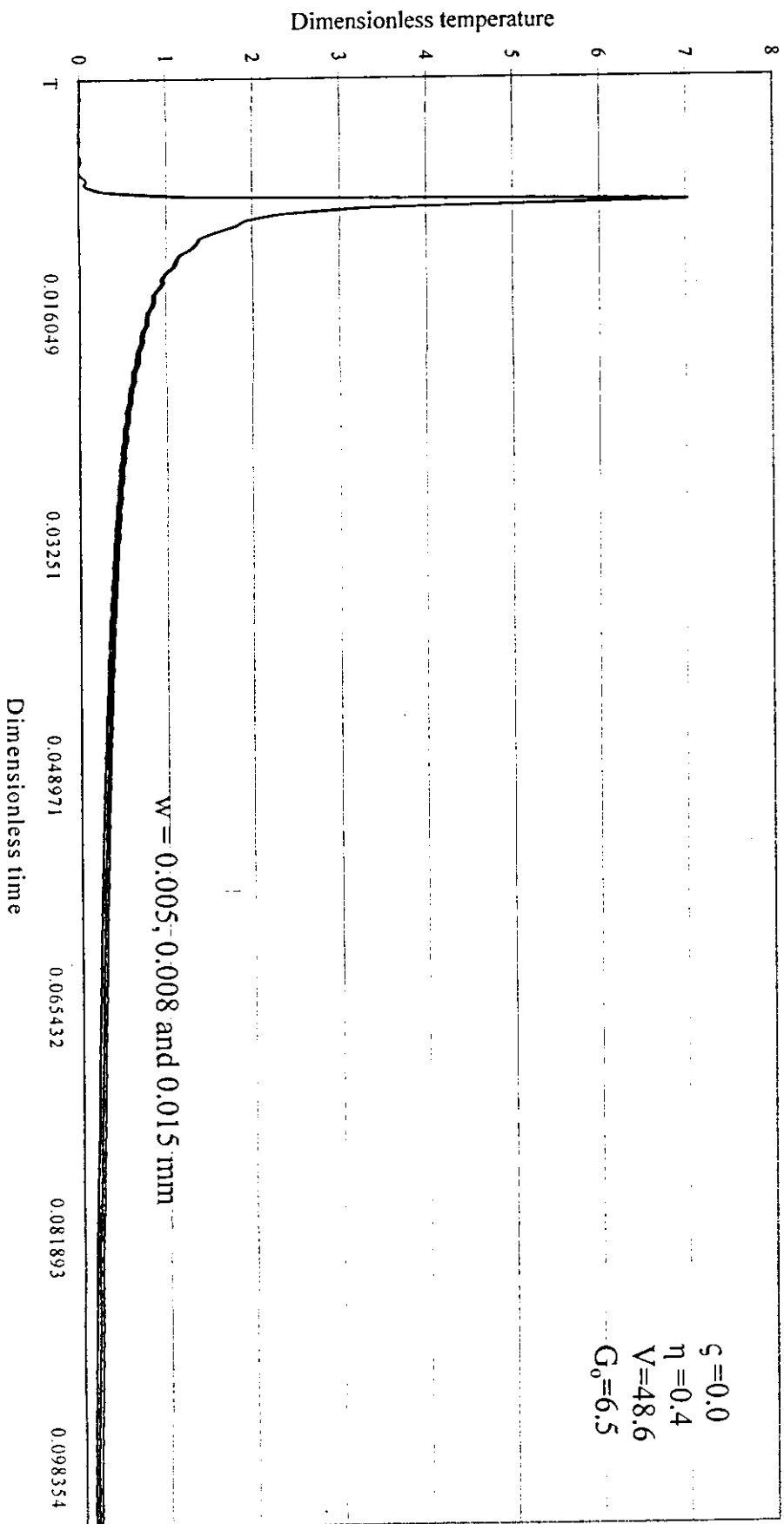


Figure (4.3.8) Residual stress distributions inside the plate at different weld speeds



Figure(4.3.9) Temperature changes at different thicknesses

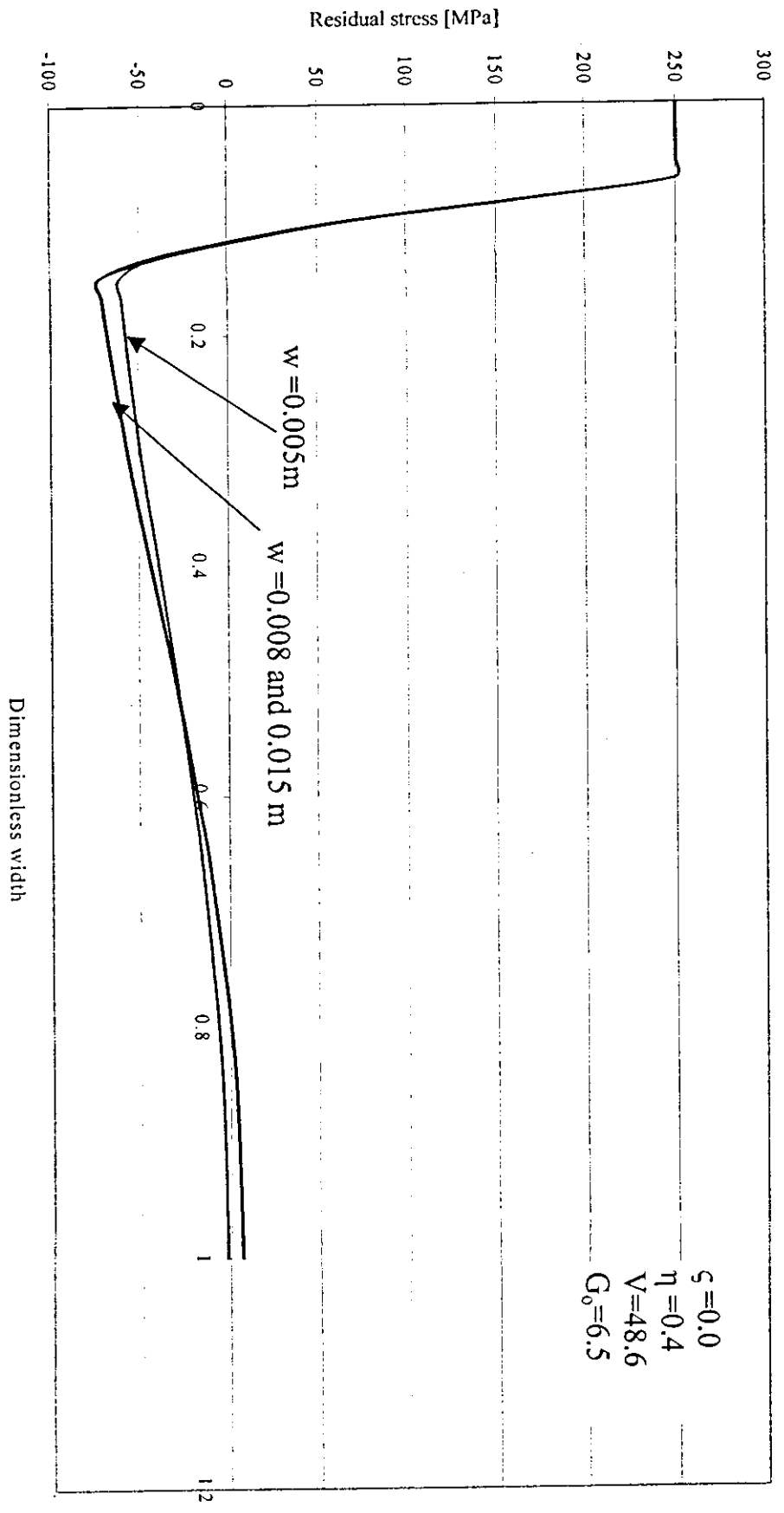


Figure (4.3.10) Residual stress distributions at different plate thicknesses

CHAPTER FIVE

CONCLUSIONS AND RECOMMENDATIONS

5.1 Conclusions

This work presents a theoretical analysis of the thermal and residual stresses inside thin plate with a moving heat source simulating arc welding.

The temperature distribution is obtained based on the energy conservation equation. The resulting equation is transformed into dimensionless form.

This new form is solved using Green's function method. A closed form solution for the temperature variation with time and space is obtained. The

thermal and residual stresses are computed based on a procedure presented originally by Tall (1964). This procedure is programmed using Fortran 77

codes. It is found that high residual tensile stresses reaching the yield limit at room temperature are produced close to the weld line after cooling of the

plates. It is also found that the thermal cycles along any transverse section are the same excepts at the edges. So the residual stress distribution at any

certain transverse section is the same.

For different heat inputs intensities, the same shape of thermal cycle is obtained but with different values. As the intensity increases, the

temperature distribution also increases and wider areas along the weld line carrying yield stresses are produced.

The effect of changing the weld speed is studied, it is found that as the weld speed decreases, the temperature inside the plate increases and the residual stresses reaching the yield limit are produced in wider areas along the welded area.

Three values of plate thickness are studied; slight effect on thermal cycles and residual stress distributions is noticed.

5.2 Recommendations

1. During the derivation of the temperature distribution equation, many assumptions were used; one of them was that the thermal properties are constant in the heat equation, considering the variation of these properties is proposed for another investigation.
2. The present work is a modeling of one-dimensional analysis, A two dimensional analysis study for the same plate is proposed for more investigations.
3. To study the effect of more welding parameters such as plate length, initial and boundary conditions, type of mounting during welding,... etc.

REFERENCES:

1. Al-Nimr, M. A. and Abou Arab, T. W., 1994. Transient Temperature Distribution Within a Flat Sheet During the Welding Process-Analytical Solution. *Heat Transfer Engineering*, Vol. 15, pp. 27-33.
2. Antunes, A., 1995. Residual Stresses in Welding; Basic Aspects. *Journal of the Brazilian Society of Mechanical Sciences*, Vol. 17, pp. 394-403.
3. Gourd, L. M., 1980. *Principles Of Welding Technology, First Edition*, ELBS, UK.
4. Masubuchi, Koichi, 1980. *Analysis of Welded Structures, First Edition*, Pergamon Press, London.
5. Olabi, A. and Hashmi, M., 1996. Stress Relief Procedures for Low Carbon Steel (1020) Welded Components. *Journal of Materials Processing Technology*, Vol. 56, pp. 552-562.
6. Ozisik, M. Necati, 1993 *Heat Conduction, Second Edition*, John Wiley and Sons. USA.
7. Radaj, Dieter, 1992. *Heat Effects of Welding*. Springer-Verlag, USA.
8. Roelens, J. B. and Multrud, F., 1996. Determination of Residual Stresses in Submerged Arc Multi-Pass Welds by Means of Numerical Simulation and Comparison with Experimental Measurements. *Welding Research Abroad*, Vol. 42, pp. 36-43.

9. Tall, Lambert, 1964. Residual Stresses in Welded Plates-A Theoretical Study. *Welding Journal*, 43 (1), 10s-23s.
10. Ueda, Yukio and Yuan, M.G., 1993. Prediction of Residual Stresses in Butt Welded Plates Using Inherent Strains. *Journal of Engineering Materials and Technology*, Transaction of the ASME Vol. 115, pp. 417-423.
11. Ueda, Yukio and Xing Xu, 1994. Simple Measuring Methods of 3-Dimensional Residual Stresses in Bead-on-Plate Welds. *Quarterly Journal of the Japan Welding Society*, Vol. 12 n4, pp.547-553.
12. Ugural, A.C., 1981. *Stresses in Plates and Shells*. McGraw-Hill, USA.
13. Yang, L. J. and Xiao, Z. M., 1995. Elastic Plastic Modeling of the Residual Stress Caused by Welding. *Journal of Materials Processing Technology*, Vol. 48, pp. 589-601.
14. Yuan, M. G. and Ueda, Yukio, 1996. Prediction of Residual Stresses in Welded T- and I-Joints Using Inherent Strains. *Journal of Engineering Materials and Technology*, Transaction of ASME 118 n2, pp. 229-34.

APPENDIX A**COMPUTER PROGRAM FOR CALCULATING THE TEMPERATURE DISTRIBUTION AT DIFFERENT TIMES**

```

PROGRAM THYSIS
INTEGER M,N,L,K,O
DOUBLEPRECISION R,ZETA,V,ETA,GO,GAMA,THETA,PHI1,PHI,S,Q
REAL E,B,P,W,T,T1,T2,INT
C*****
C V: NORMALIZED VELOCITY
V=48.6
C GAMA:(BIL+BIU)
GAMA=-8.307692308
C GO=NORMALIZED HEAT GENEARTION
GO=6.5
C R:ASPECT RATIO=H/L
R=5.
C*****
C ZETA:X/L
ZETA=.00
C ETA:Y/L
ETA=1.0
C*****
C T1 :NORMALIZED INITAL TIME
T1=0
C T2 :NORMALIZED FINAL TIME
T2= R/V
C INT :INTERVAL OF TIME
INT=. 000578704
FINALTIME=(T2-T1)/INT+INT
C*****
PHI=0
PHI1=0
THETA=0
C*****
OPEN (2,FILE = 'OUTPUT.TXT' .STATUS='OLD')
C*****
WRITE (2, *)' T THETA'
DO 15 O=1.FINALTIME
M=0.0
THETA=0.0
PHI1=0.0
PHI=0.0
N=0.0000
C*****
DO 10 L=1.300
DO 20 K=1.300
C*****

```

```

S=(B(M)**2+E(N)**2-GAMA)
Q=E(N)*V
C*****
PHI1=GO*(P(B(M))*W(E(N))/(S**2+Q**2))
+ *DCOS(B(M)*ZETA)*DCOS(E(N)*ETA)
+ *(Q*DSIN(Q*T)+S*DCOS(Q*T)-S*DEXP(-S*T))

PHI=PHI+PHI1
C*****
N=N+1
PHI1=0
20 CONTINUE
C*****
M=M+1
N=0.00000000
THETA=THETA+PHI
PHI=0
10 CONTINUE
C*****
WRITE(2,7) T,THETA
7 FORMAT(F9.6,4X,F8.5)
T=T+INT
15 CONTINUE
END
C*****
REAL FUNCTION B(M)
B=M*(22/7.0)
RETURN
END
C*****
REAL FUNCTION E(N)
REAL R
R=5.0
E=N*(22/7.0)/R
RETURN
END
C*****
REAL FUNCTION P(X)
IF (X.EQ.0) THEN
P=1
ELSE
P=2
ENDIF
RETURN
END
C*****
REAL FUNCTION W(Y)
REAL R
R=5.0
IF (Y.EQ.0) THEN

```


APPENDIX B**COMPUTER PROGRAM FOR CALCULATING THE PHYSICAL
PROPERTIES AT DIFFERENT TEMEPRAURE VALUES**

```

PROGRAM COEFFICENTS
REAL ALPHA,YOUNG,SEGMA,TEMP
10 PRINT*,'ENTER THE VALUE OF TEMPERATURE'
READ*, TEMP
IF (TEMP .GT.888) THEN
SEGMA=0.0
YOUNG=0
ALPHA=0
GOTO 20
ENDIF
C*****
A1=250.00
B1=0.068057552
C1=-0.0007946605
D1=+0.00000045579904
C*****
A2=199.99891
B2=-0.034206869
C2=-0.00001239125
D2=-0.00000020535626
C*****
SEGMA=A1+B1*TEMP+C1*TEMP**2+D1*TEMP**3
YOUNG=A2+B2*TEMP+C2*TEMP**2+D2*TEMP**3
IF (TEMP.LT.732)THEN
C*****
A3=10.178461
B3=+0.019198913
C3=-0.000018752367
D3=+0.0000000078132847
C*****
ELSE
A3=931.82612
B3=-3.3304901
C3=+0.0038835515
D3=-0.0000014633018
ENDIF
ALPHA=A3+B3*TEMP+C3*TEMP**2+D3*TEMP**3
20 PRINT*,' SEGMA=',SEGMA,' YOUNG=',YOUNG,' ALPHA=',ALPHA
GOTO 10
END

```

529020

APPENDIX C**COMPUTER PROGRAM FOR CALCULATING THE TEMPERATURE DISTRIBUTION AT DIFFERENT TIMES ALONG CERTAIN SECTION ON THE PLATE**

```

PROGRAM THYSIS
INTEGER M,N,L,K
Real R,ZETA,V,ETA,GO,GAMA,THETA,PHI1,PHI,S,Q
REAL E,B,P,W,T,INT, displ

C*****
C  V: NORMALIZED VELOCITY
  V=48.6
C  GAMA:(BIL+BIU)
  GAMA=-8.307692308
C  GO=NORMALIZED HEAT GENEARTION
  GO=6.5
C  R:ASPECT RATIO=L/H
  R=5.
C*****
C  ZETA:X/L
  ZETA=0.0
C  ETA:Y/L
  ETA=0.4
C*****
C  T1 :NORMALIZED INITAL TIME
  T=0.04197530826
  T1=0.00
C  T2 :NORMALIZED FINAL TIME
  T2= R/V
C  INT :INTERVAL OF TIME
  INT=0.00041152263
  FINALTIME=(T2-T1)/INT+INT
C*****
  PHI=0
  PHI1=0
  THETA=0
C*****
  OPEN (2,FILE = 'MOUTPUT3.TXT' ,STATUS='OLD')
C*****

DO 15 O=1.FINALTIME
WRITE(2,*) 4860*T
DO 100 II=1.28
M=0.0
THETA=0.0
PHI1=0.0
PHI=0.0

```

```

N=0.0000
C*****
DO 10 L=1,500
DO 20 K=1,500
C*****
S=(B(M)**2+E(N)**2-GAMA)
Q=E(N)*V
C*****
PHI1=GO*(P(B(M))*W(E(N))/(S**2+Q**2))
+ *DCOS(B(M)*ZETA)*DCOS(E(N)*ETA)
+ *(Q*DSIN(Q*T)+S*DCOS(Q*T)-S*DEXP(-S*T))

PHI=PHI+PHI1

C*****
N=N+1
PHI1=0
20 CONTINUE
C*****
M=M+1
N=0.0
THETA=THETA+PHI
PHI=0.0
10 CONTINUE
C*****
WRITE(2,*)3*ZETA,300*THETA+300-273
IF (ZETA.LE..33333333) THEN
DISPL=0.01666666666667
ELSEIF ( ZETA.LE..6666666664) THEN
DISPL=0.066666666664
ELSE
DISPL=0.1666666666667
ENDIF
ZETA=ZETA+DISPL
100 CONTINUE
ZETA=0.0
T=T+INT
15 CONTINUE
END
C*****

REAL FUNCTION B(M)
B=M*(22/7.0)
RETURN
END
C*****
REAL FUNCTION E(N)
REAL R
R=5.0
E=N*(22/7.0)/R

```

```
RETURN  
END
```

```
C*****
```

```
REAL FUNCTION P(X)  
IF (X.EQ.0) THEN  
P=1  
ELSE  
P=2  
ENDIF  
RETURN  
END
```

```
C*****
```

```
REAL FUNCTION W(Y)  
REAL R  
R=5.0  
IF (Y.EQ.0) THEN  
W=1/R  
ELSE  
W=2/R  
ENDIF  
RETURN  
END
```

APPENDIX D**COMPUTER PROGRAM FOR CALCULATING THE RESIDUAL STRESSES
INSIDE THE THIN PLATE**

```

PROGRAM RESIDUAL
REAL T(290),X(100),TEMP(100),TAVE(100),DT(100),N,TEMPPRV(100),
+ DP(100),SEGMACAL(100),SEGMA0(100),SEGMAEQU,DB(100),SEGPRV(100)
+,SEGMASIGN
TINI=27
N=0
IMAX=28
SEGMAEQU=0.0
SEGMASIGN=0.0
OPEN(2,FILE='MOUTPUT3.TXT',STATUS='OLD')
OPEN(3,FILE='MOUTPUT33.TXT',STATUS='OLD')
DO 70 I=1,IMAX
TEMPPRV(I)=TINI
70 CONTINUE
DO 80 K=1,251
READ(2,*) T(K)
N=0.0
DO 100 I=1,IMAX
READ(2,*) X(I),TEMP(I)
100 CONTINUE
DB(1)=(X(2)-X(1))/2.
DB(IMAX)=(X(IMAX)-X(IMAX-1))/2.
DO 90 I=2,(IMAX-1)
DB(I)=(X(I+1)-X(I-1))/2.
90 CONTINUE
DO 110 I=1,IMAX
TAVE(I)=(TEMP(I)+TINI)/2.
DT(I)=(TEMP(I)-TEMPPRV(I))
SEGMACAL(I)=-1/1000.*ALPHA(TAVE(I))*YOUNG(TAVE(I))*DT(I)
110 CONTINUE
140 DO 120 I=1,IMAX
IF (SEGMA(TEMP(I)) .GE. SEGMACAL(I)) THEN
SEGMA0(I)=SEGMA(TEMP(I))
ELSE
SEGMA0(I)=SEGMACAL(I)+SEGPRV(I)+SEGMAEQU
ENDIF
IF((SEGMA0(I) .LE. 0.0).AND.(SEGMA0(I).LE. SEGMA(TEMP(I)))) THEN
SEGMA0(I)=SEGMA(TEMP(I))
ELSEIF((SEGMA0(I).GT. 0.0).AND.(SEGMA0(I).GE. ABS(SEGMA(TEMP(I))))
+ )THEN
SEGMA0(I)=-1*SEGMA(TEMP(I))
ENDIF
120 CONTINUE
IF (N .EQ. 50 000) THEN

```

```

PRINT*,'
PRINT*,'***** NO OF ITERATIONS EXCEEDED****'
DO 125 I=1,IMAX
PRINT*,'RESIDUAL STRESSSS AT T('2*K-2,')=',SEGMA0(I)
PRINT*,'SUM OF FORCES AT T('2*K-2,')=',SUM
PRINT*,'N=',N
125 CONTINUE
GOTO 150
ENDIF
SUM=0.0
DO 130 I=1,IMAX
DP(I)=SEGMA0(I)*DB(I)
SUM=SUM+DP(I)
130 CONTINUE
IF (SUM .GE. .3) THEN
SEGMA0(I)=SEGMA0(I)-.005
ELSEIF (SUM .LT.0.0) THEN
SEGMA0(I)=SEGMA0(I)+.005
ENDIF
IF (ABS(SUM) .LT. .005) THEN
DO 135 I=1,IMAX
PRINT*,'RESIDUAL STRESSSS AT T('2*K-2,')=',SEGMA0(I)
WRITE (3,*)'RESIDUAL STRESSSS AT T('2*K-2,')=',SEGMA0(I)
135 CONTINUE
WRITE (3,*)'SUM OF FORCES AT T('2*K-2,')=',SUM
PRINT*,'N=',N

PRINT*,'SUM OF FORCES AT T('2*K-2,')=',SUM
PRINT*,'_____
ELSE
N=N+1
PRINT*,'NO OF ITERATIONS=',N
SEGMA0(I)=SEGMA0(I)+SEGMA0(I)*SEGMA0(I)
GOTO 140
ENDIF
SEGMA0(I)=0.0
SUM=0.0
150 DO 170 I=1,IMAX
SEGPRV(I)=SEGMA0(I)
TEMPPRV(I)=TEMP(I)
170 CONTINUE
80 CONTINUE
STOP
END
C*****
REAL FUNCTION ALPHA(TAVE)
IF(TAVE.GT.888)THEN
A3=0
B3=0
C3=0

```

```

D3=0
ELSEIF (TAVE .LT.732)THEN
A3=10.178461
B3=+0.019198913
C3=-0.000018752367
D3=+0.0000000078132847
ELSEIF(TAVE.LT.888) THEN
A3=931.82612
B3=-3.3304901
C3=+0.0038835515
D3=-0.0000014633018
ENDIF
ALPHA=A3+B3*TAVE+C3*TAVE**2+D3*TAVE**3
RETURN
END
C*****
REAL FUNCTION YOUNG(TAVE)
IF(TAVE.GT.888)THEN
A2=0
B2=0
C2=0
D2=0
ELSE
A2=199.99891
B2=-0.034206869
C2=-0.00001239125
D2=-0.00000020535626
ENDIF
YOUNG=A2+B2*TAVE+C2*TAVE**2+D2*TAVE**3
RETURN
END
C*****
REAL FUNCTION SEGMA(TEMP)
IF(TEMP.GT.888)THEN
A1=0
B1=0
C1=0
D1=0
ELSE
A1=249.00
B1=0.068057552
C1=-0.0007946605
D1=+0.00000045579904
ENDIF
SEGMA=-1*(A1+B1*TEMP+C1*TEMP**2+D1*TEMP**3)
RETURN
END

```

ملخص

التغيرات الانتقالية للاجهادات الحرارية والاجهادات المتبقية الناتجة عنها داخل
صفحة رقيقة اثناء عمليات اللحام

اعداد

ماهر احمد دعاس

المشرف

الدكتور ناصر الحنيطي

المشرف المشارك

الدكتور محمد النمر

تم دراسة التغيرات التقلية للاجهادات الحرارية والاجهادات المتبقية في صفحة معدنية رقيقة
الناتجة عن عمليات اللحام. تم إيجاد التوزيع الحراري داخل الصفحة بافتراض ظروف محيطية معينة
تحليلياً. بعد ذلك تم حساب الاجهادات الحرارية وبعدها تم حساب الاجهادات المتبقية الناتجة عنها، و
التي تبقى داخل الصفحة بعد برودها، بواسطة الطريقة التي قدمها العالم "تال" عام ١٩٦٤م وتم تقديم
النتائج بواسطة الأشكال الرسومية.

تم استنتاج ان لسرعة اللحام وشدة المصدر الحراري المستخدم الأثر الكبير في عملية تكوين
الاجهادات المتبقية.